



UNIVERSITY OF BIRMINGHAM

**Identifying protein markers of skeletal muscle small
extracellular vesicle secretion during exercise**

Student ID:

Supervisor: Dr Martin Whitham

Word Count: 15,670

School of Sport, Exercise and Rehabilitation Sciences

UNIVERSITY OF
BIRMINGHAM

University of Birmingham Research Archive

e-theses repository

This unpublished thesis/dissertation is copyright of the author and/or third parties. The intellectual property rights of the author or third parties in respect of this work are as defined by The Copyright Designs and Patents Act 1988 or as modified by any successor legislation.

Any use made of information contained in this thesis/dissertation must be in accordance with that legislation and must be properly acknowledged. Further distribution or reproduction in any format is prohibited without the permission of the copyright holder.

Abstract

Extracellular Vesicles (EVs) are membranous particles which act as a method of cellular communication between cells and tissues through the transfer of lipids, proteins, and RNA cargo. Exosomes are a subpopulation of EV which are derived from the cell cytosol, meaning the packing of proteins into exosomes is pre-determined intracellularly based on the origin (i.e., adipose vs muscle) and condition (i.e., exercise vs sedentary) from which they are influenced, making them interesting candidates for biomarker discovery. During exercise, there is an acute rapid release of small EVs (sEVs), consisting of both exosomes and small microvesicles, into the circulation which has been proposed to provide a method of tissue crosstalk during exercise (Whitham et al., 2018). Due to the lack of a methodological approach that allows for the clear separation of various tissue derived sEVs, the contribution of skeletal muscle to the increase in systemic sEVs during exercise is unclear. In this regard, whether skeletal muscle sEVs play a role in tissue crosstalk during exercise is not known.

With the aim of identifying novel candidate protein markers of skeletal muscle sEV secretion, the present study curated, re-analyzed and overlaid currently available proteomic datasets regarding muscle derived EV bound proteins that are also exercise responsive *in vitro* and *in vivo*; recognizing ANXA6 and CD44 as candidate protein markers of muscle sEV secretion. Immunoblotting of ANXA6, CD44 and alpha sarcoglycan (SGCA), a previously proposed muscle specific sEV marker, amongst several different cell lines revealed that ANXA6 and CD44 were enriched ($P < 0.05$) but not specifically expressed in C2C12 myotube sEVs. SGCA however, was highly unique to myotube sEVs compared to other cell lines ($P < 0.05$). Noticeably, *in vitro* stimulation by ionomycin (IM) caused a ~4-fold increase in the secretion of sEVs from

C2C12 myotubes detected by nanoparticle tracking analysis (NTA), of which these affects were reflected by increases in ANXA6+ ($P < 0.05$, 158.29%) and CD44+ ($P < 0.05$, 180.69%) sEVs but not SGCA ($P = 0.6244$, 6.58%). This suggests that the secretion of sEVs from muscle might be somewhat calcium regulated. Mechanical contraction, induced by electrical pulse stimulation (EPS), did not produce similar results. Seemingly EPS as a model is limited in its ability to generate sufficient calcium transients in C2C12s (Olsson et al., 2015), which might explain this response. Finally, acute high intensity interval exercise (HIIE) recapitulated the increase in systemic sEVs previously reported by others (Fruhbeis et al., 2015; Whitham et al., 2018; Brahmer et al., 2019; Vanderboom et al., 2021) as indicated by the increase in CD9+ ($P < 0.05$, 28.28%), CD63+ ($P < 0.05$, 68.64%) and CD81+ ($P < 0.05$, 13.16%) sEVs immediately post exercise. However, these changes were only observed in CD44+ sEVs isolated by immunomagnetic precipitation (IMP) ($P < 0.05$, 879.84%) and not ultracentrifugation (UC) ($P = 0.1002$, 33.82%) suggesting that the purity of isolation forms part of the observed changes in specific protein markers. Overall, it is unclear as to whether skeletal muscle sEVs are liberated into the circulation with acute exercise and more research is needed to conclude the confidence of protein markers including ANXA6 and CD44 as sufficient markers of skeletal muscle sEV release in the circulation. Similarly, calcium influx into the sarcolemma with contraction might present a method of sEV secretion *in vivo* and as such warrant further investigation into the mechanisms regulating EV biogenesis and secretion from skeletal muscle. Finally, the present study highlights how the use of currently available proteomic data can be adopted to inform targeted methods in novel protein marker discovery and validation.

Acknowledgements

I would firstly like to thank Dr Martin Whitham for his support and advice over the last 2 years. Without his encouragement and continued guidance, I would not have been able to achieve what I have in this project. Secondly, I would also like to thank Dr Alex Seabright and Dr Luke McIvennan for tutoring and mentoring me over the course of this project and for being great friends to me throughout my time in the Tissue Crosstalk lab, without them I would not be the researcher I am today. Finally, a huge thank you to all my friends and family for their relentless moral support over the course of this challenging year.

Declarations

Firstly, thank you to Luke McIvennan who performed the size exclusion chromatography (SEC) isolations and nanoparticle tracking analysis (NTA) used in the present study. Secondly, to the Lucas group who designed and ran the high intensity exercise protocol and took the human blood samples. Lastly, to Hannah Park who completed the ExoView preparation and analysis of *in vivo* exercise samples.

Table of Contents

1. Introduction

- 1.0** Exercise and health
- 1.1** Exercise and tissue crosstalk
- 1.2** Skeletal muscle in exercise, health, and disease
- 1.3** Extracellular Vesicles (EVs)
- 1.4** Current limitations in EV isolation
- 1.5** Exercise and sEVs
- 1.6** Functional role of sEVs in tissue crosstalk during exercise
- 1.7** Skeletal muscle derived sEVs
- 1.8** The relevance of protein markers in tissue specific EV detection
- 1.9** The use of global proteomics in skeletal muscle EV protein marker discovery

2. Methods and Material

- 2.0** Proteomic Analysis
- 2.1** Cell line protocol
- 2.2** *In vitro* stimulation of C2C12 myotubes
- 2.3** High Intensity Interval Exercise (HIIE)
- 2.4** Isolation of sEVs
- 2.5** Sample preparation and Immunoblotting
- 2.6** Nanoparticle Tracking Analysis (NTA)
- 2.7** ExoView
- 2.8** Statistical analysis

3. Results

- 3.0** Proteomic overlay analysis reveals ANXA6 and CD44 as candidate skeletal muscle derived exercise responsive sEV markers

- 3.1 ANAX6 and CD44 are components of myotube derived sEVs
- 3.2 ANXA6 and CD44 are highly abundant but not unique to myotube sEVs
- 3.3 ANXA6 and CD44 are calcium responsive markers of sEV secretion from C2C12 myotubes stimulated *in vitro*
- 3.4 Selective isolation of tetraspanin positive sEVs highlights CD44 as a potential candidate marker of sEV secretion with exercise *in vivo*

4. Discussion

- 4.0 Proteomic overlay highlights ANXA6 and CD44 and novel candidate markers of skeletal muscle EV secretion with exercise
- 4.1 Advantages of combining proteomics and targeted methods for skeletal muscle EV protein marker discovery
- 4.2 SGCA is a highly unique myotube EV marker
- 4.3 Syntenin-1 is a better candidate putative marker of exosomes compared to canonical tetraspanin marker CD9
- 4.4 Myotube secretion of sEVs is calcium sensitive *in vitro*
- 4.5 HIIE causes an increase in circulating tetraspanin positive sEVs
- 4.6 The purity of isolation method effects the clarity of observed changes in sEV marker dynamics with HIIE *in vivo*
- 4.7 SGCA may represent a non-exercise responsive marker of skeletal muscle sEV secretion
- 4.8 The potential role of ANXA6 and CD44 in sEVs secreted from myotubes
- 4.9 Local and/or distal crosstalk of skeletal muscle EVs: A need for further research
- 4.10 Conclusion

5. References

6. Supplementary

1. Introduction

1.0) Exercise and health

Regular physical activity is well known to result in multiple physiological benefits that aid in the suppression of chronic pathological diseases while improving mental and physical health and wellbeing (Warburton, Nicol & Bredin, 2006; Fox, 2007). The multisystemic benefits of regular exercise can be characterized by reductions in adiposity, improvements in skeletal muscle function and cardiorespiratory fitness (Hawley et al., 2014). All of which are attributable to minute physiological alteration brought about by the repetitive stress of physical activity that exceeds our bodies nature homeostasis. With this, our bodies adapt over time to deal with such demands. As a result, regular physical activity is one of the best prescribed medicines against metabolic diseases such as type 2 diabetes mellitus (T2DM), obesity and cardiovascular disease (CVD) (Warburton, Nicol & Bredin 2006). Additionally, regular physical activity has also been shown to mitigate age related cognitive decline and disease development (Intlekofer & Cotman, 2013) and has been strongly linked to the suppression of specific cancers (Colditz et al., 1997; Friedenreich, 2011). In turn, regular physical activity is a major contributor to improving overall health and mortality over a lifetime (Warburton, Nicol & Bredin, 2006; Gill & Malkova, 2016).

1.1) Exercise and tissue crosstalk

The mechanisms that regulate the multisystemic adaptive response of physical activity rely on a complex network of signaling molecules functioning intracellularly and extracellularly. Recent work has led to the adoption of the term, 'exerkines' which refers to humeral factors (peptides, metabolites and RNAs) that are secreted into the circulation in response to acute or chronic exercise. Exerkine is an umbrella term that

encapsulates the secretion of humeral factors from all tissues around the body. More specifically, myokines, secreted from muscle; hepatokines, secreted from liver; adipokines, secreted from adipose, are some of the more extensively studied exerkinines due to their potential role in exercise induced tissue crosstalk (Romacho et al., 2014; Severinsen & Pedersen, 2020; Jensen-Cody & Potthoff, 2021); although theoretically any tissue and/or cell can add to the exercise secretome, emphasizing the complexity of exerkinine identification and tissue crosstalk during exercise. As such, it has been hypothesized that the adaptive benefits seen with regular physical activity are in part, due to the release and uptake of exerkinines that regulate multisystemic benefits in multiple tissues around the body (Whitham & Febbraio, 2016; Magliulo et al., 2021).

1.2) Skeletal muscle in exercise, health, and disease

Skeletal muscle makes up the largest organ in the human body amounting to ~40% of total body weight (Frontera & Ochala, 2014). It is primarily made up of a vast array of muscle fibers containing contractile structures which together produce movement and aid posture. Skeletal muscle is plastic and can change overtime with alterations in the balance between protein synthesis and degradation influenced largely by levels of physical activity (Fluck & Hoppeler, 2003). A loss of skeletal muscle mass, for example due to sedentarism alongside malnutrition can emphasize the progression of multiple chronic diseases (Booth, Roberts & Laye, 2012). For the duration of physical activity, skeletal muscle fibers are exposed to metabolic and mechanical stresses by which acute metabolic regulation, substrate oxidation, protein metabolism and autophagy, cytoskeletal mechanics, and transcriptional control of metabolism, synchronize muscle dynamics during and after physical activity (Frontera & Ochala, 2014). As a result, a

vast heterogenous pool of myokines are released that can alter the physiology of other cells and tissues around the body (Pedersen & Febbraio, 2012; Kirby, Chaillou & McCarthy, 2016). The identification of skeletal muscle as an endocrine organ (Peddersen & Febbraio, 2012) and the fact it drastically changes its metabolic status during exercise makes it likely to be a major contributing source in the circulating exercise secretome. Myokines including interleukin-6 (IL-6), irisin, myonectin, meteorin-like protein, and fibroblast growth factor 21 are a few of many that are released from skeletal muscle in response to exercise or muscular contraction (Whitham & Febbraio, 2016). The secretion of these myokines during exercises induces alterations in the gene and protein expression of target cells (Severinsen & Pedersen, 2020). In this regard, it is hypothesized that many of these secretory factors released from skeletal muscle during exercise partially regulate the benefits of physical activity in acute and chronic disease suppression (Whitham & Febbraio, 2016).

Until recently, exerkine and myokine release by cells during exercise only regarded the classical secretory pathway. By this method, newly synthesized proteins containing a signal peptide (typically at the N-terminus) or through the addition of a signal peptide during post-translational modification, are destined for translocation to the endoplasmic reticulum and Golgi secretory pathway. In doing this, proteins are targeted to the cellular membrane to either be secreted into the extracellular space or embedded in the phospholipid bilayer (Burgess & Kelly, 1987; Owji et al., 2018). However, many peptides and signaling molecules, including exerkines and myokines do not contain a signaling peptide and therefore can be secreted into the extracellular space via extracellular vesicles (EVs), otherwise termed non-classical secretion (Bendtsen et al., 2004). This provides a means for cellular crosstalk through the

transfer of signaling molecules regardless of signal peptide and/or classical secretion (Nickel & Seedorf, 2008).

1.3) Extracellular Vesicles (EVs)

EVs are membrane-bound nanoparticles produced by most, if not all, cell types with a functionality of cellular communication. The heterogenous nature of EVs makes characterization challenging, therefore, broader terms have been designated to distinguish subpopulations based on their size, densities, biogenesis, and cargo. Disregarding apoptotic bodies, EVs can be categorized vaguely into microvesicles (~50-1000nm in diameter) and exosomes (40-150nm in diameter) (Kalluri & LeBleu, 2020). Microvesicles are formed from the clustering of cytosolic contents around the inner membrane, eventually becoming enwrapped in bilayer, pinching or blebbing off the cell (Raposo & Storch, 2013). Conversely, exosome biogenesis originates intracellularly from the endocytic pathways from which cytosolic materials are internalized and directed to either the lysosomal pathway or the cellular membrane. The formation of exosomes is extremely complex and is yet to be fully elucidated, however previous reports have covered it extensively (Raposo & Storch, 2013; Akers et al., 2013; Edgar, 2016; Lässer, Jang & Lotvall, 2018). In brief, exosomes are assembled from the endosomal compartment of cells, consisting of an invagination of the phospholipid bilayer by which the early endosome is formed. Early endosomes become contained within multivesicular bodies (MVBs) via the aid of endosomal sorting complexes required for transport (ESCRT), from which they are termed intraluminal vesicles (ILV). MVBs carrying ILVs are either destined for degradation of their contents by lysosomes in the lysosomal pathway, or they can fuse with the cellular membrane, secreting exosomes by exocytosis. Tetraspanin proteins CD9,

CD63 and CD81 are believed to be involved in early ILV formation, while the ESCRT complex of proteins, including tumour susceptibility gene 101 (TSG101), Syntenin-1 and apoptosis-linked gene 2 interacting protein X (ALIX), cooperate to regulate ILV formation, MVB budding and the secretion of the exosome (Raposo & Storch, 2013; Akers et al., 2013; Edgar, 2016; Lasser, Jang & Lotvall, 2018). From this, a multitude of these proteins are incorporated into the secreted exosome and as such, are used as markers in their identification. After their secretion from the host cell, exosomes merge with the plasma membrane or are taken up by the target cell for degradation of their luminal contents. Uptake of exosomes is dependent on the interaction between a whole host of membranous surface receptors, glycoproteins, lipids, and binding complexes (i.e., integrins, tetraspanins, lipid rafts) which determine the uptake and/or internalization of exosomes by the target cell (Mulcahy, Pink & Carter, 2014). Hereon, exosomes transfer their luminal contents into the target cell. The composition of exosomes has been detailed in Figure 1.

The formation, transportation, and delivery of EVs provides a system for cellular communication in an autocrine, paracrine, and endocrine fashion; intriguingly, one that protects its cellular contents from harsh environments, such as the circulation. Notably, EVs have been reported in multiple biological fluids and are thought to be secreted by all cell types, as highlighted in a review by Doyle et al., (2019); suggesting that utilization of this method for cellular communication and transportation mediates whole body homeostasis. The intracellular biogenesis of exosomes presents the cargoing of specific cellular components linking both the cell origin and target cell through the transfer of luminal lipids, proteins, metabolites, RNAs (the most extensively researched being mRNA, and miRNA) and DNAs (Raposo & Storch, 2013; Akers

et al., 2013; Lasser, 2015; Edgar, 2016; Doyle et al., 2019). The unique packaging of luminal cargo between cells and amongst various physiological and pathological conditions results in the secretion of heterogeneous subpopulations of exosomes that are specific to the cell of origin and the condition from which they are influenced (Raposo & Storch, 2013). This makes them extremely interesting candidates in the context of biomarker discovery (Properzi, Logozzi & Fais, 2013; Lin et al., 2015). Already, research has begun to elucidate the clinical relevance of proteins and miRNAs as exosomal biomarkers in the detection of cancers (Rak, 2013; Soung et al., 2017; Wong & Chen, 2019), CVD in adults (Bei et al., 2017; Zamani et al., 2019; Moreira-Costa et al., 2021) and children (Khalyfa & Gozal, 2014), T2DM (Jones et al., 2017; Echner, Erdbrugger & Malin, 2018), renal disease (Zhou et al., 2008), inflammation (Console, Scalise & Indiveri, 2019), age-related cognitive decline (Rani et al., 2017) and many other pathological conditions (Lin et al., 2015).

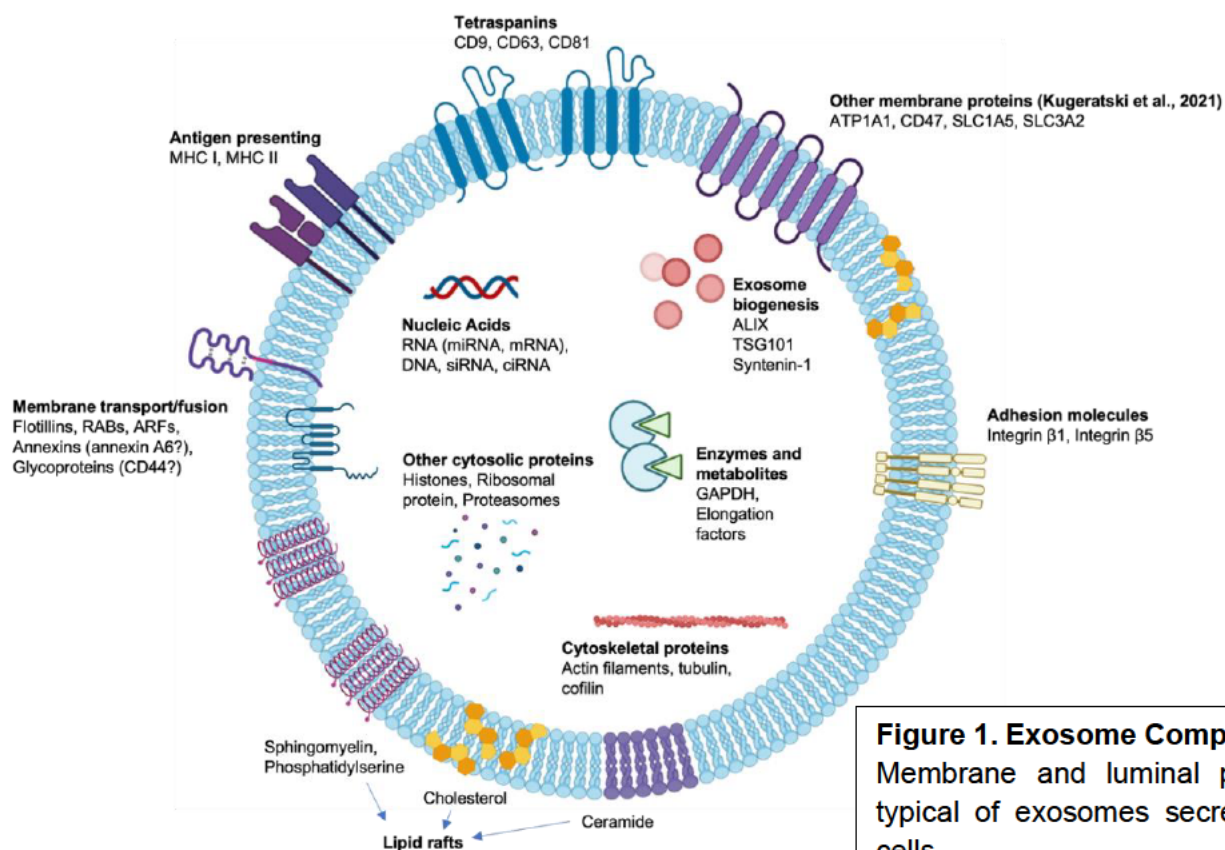


Figure 1. Exosome Composition
Membrane and luminal proteins typical of exosomes secreted by cells.

1.4) Current limitations in EV isolation

To date, there is no gold standard method of vesicle isolation that distinctly allows separation of subpopulations of EVs either based on biogenesis (exosome vs microvesicle) or origin (i.e., adipose vs muscle). Techniques for EV separation can be broadly categorized into five groups. These constitute; density/sedimentation (density gradient; DG, ultracentrifugation; UC), immunoaffinity and microfluidics-based capture (immunomagnetic precipitation; IMP), size exclusion (size exclusion chromatography; SEC, ultrafiltration; UF) and volume exclusion (precipitation) (Witwer et al., 2013). Simply, EVs are isolated and arranged based on size, density, solubility, and antigen binding. Current methodological strategies for EV isolation do not allow for the absolute removal of contaminant particles and/or aggregates. For example, strategies which aim to separate EVs from complex biofluids, such as blood, are highly susceptible to co-isolation of contaminants due to the large abundance of lipoproteins, plasma derived vesicles (i.e., platelet vesicles) and proteins (i.e., albumin), chylomicrons, immunoglobulins, and other macromolecules (Witwer et al., 2013). As such, methodological approaches that aim to generate higher purity (i.e., SEC, DG) of separation typically sacrifice protein and particle yield due to the repeated filtration of unwanted contaminants also sacrificing EV isolation. Conversely, approaches which aim to generate yield (i.e., UC, UF) are limited by purity (Brennan et al., 2020). Therefore, due to a lack of methodological standardization for EV isolation, the chosen method(s) of isolation is/are influenced largely by the sample, conditions, and downstream analysis (i.e., immunoblotting, PCR, flow cytometry) (Erdburger & Lannigan, 2015) such that the choice of EV purification and characterization should be carefully considered based on the desired outcome (i.e., discovery research,

diagnostic research, preparative research) to prevent false interpretation and discovery (Witwer et al., 2013).

The heterogeneity of EV secretion, coupled with the current inability in technological methods to separate exosome and smaller microvesicle populations due to their similar biophysical properties (i.e., size, density, sedimentation), has led to debates on appropriate nomenclature. To clarify, here, the term 'small EVs' (sEVs) will be adopted in reference to exosome and small microvesicle isolations, whereas the term 'EVs', will be used in referral to all exosome and microvesicle populations.

1.5) Exercise and sEVs

It is well considered that an acute bout of exercise triggers the secretion of sEVs into the circulation (Fruhbeis et al., 2015; Whitham et al., 2018; Brahmer et al., 2019; Vanderboom et al., 2021; Kobayashi et al., 2021); which will be termed here as the exercise-sEV response. This was first shown by Fruhbeis et al., (2015) who illustrated that an incremental bout of running or cycling induced a significant increase immediately post exercise in the total number of circulating sEVs identified by nanoparticle tracking analysis (NTA); a method of analyzing particle size distribution (~20n-1000nm in diameter) and concentration within a sample, alongside immunoblotting for sEV markers HSP/Hsc70 and Flotillin 1 (Flot1) as well as canonical exosome marker TSG101. Similar results were observed in a later study by Brahmer et al., (2019), who adopted flow cytometry (FC) coupled with antibody capture bead analysis, showing that incremental cycling in trained male athletes caused and increase in circulating exosomal tetraspanin markers CD9, CD63 and CD81 during and immediately post exercise. Notably, the expression of these three tetraspanins began to increase at submaximal exercise intensities, prior to increases in circulating

lactate (Brahmer et al., 2019), suggesting that sEV secretion into the circulation may occur from more immediate exercise responses. In accordance with work by Vion et al., (2013) which highlights that shear stress regulates EV release from endothelial cells and platelets, it is fathomable that exercise induced increases in shear stress contributes to this rapid release of sEVs into the circulation. However, other early indicators of exercise such as muscular contraction, increased heart rate and ventilation may also contribute however the exact mechanisms by which this occurs have yet to be elucidated.

In a more comprehensive analysis, Whitham et al., (2018) and Vanderboom et al., (2021) both adopted mass-spectrometry based proteomics to evaluate changes in the sEV proteome with a bout of high intensity aerobic cycling exercise (60 minutes incremental exercise to exhaustion, and 3 x 4 minutes high intensity intervals ~90%VO₂max, respectively). Vanderboom et al., (2021) reported significant upregulation of 321 sEV associated proteins immediately post exercise, whereas Whitham et al., (2018) identified a total of 322 proteins significantly different between exercise and rest. Notably, both groups adopted different isolation methods (Vanderboom et al., adopted SEC whereas Whitham et al., used UC), yet both showed similar responses, suggesting that changes in the EV proteome and particle count (detected by NTA in both) indicative of the acute exercise-sEV response, occurs regardless of isolation method. In a similar fashion, both groups showed a relatively transient effect of exercise on sEV secretion, highlighting the return of most upregulated proteins back to baseline levels within 3 (Vanderboom et al., 2021) and 4 hours (Whitham et al., 2018) after exercise cessation. Interestingly, treadmill running resulted in a sustained elevation in NTA detected sEVs up to ~6 hours (Fruhbeis et

al., 2015), whereas cycling exercise appears to induce a slightly more acute response of between ~90 minutes to ~4 hours (Fruhbeis et al., 2015; Whitham et al., 2018; Vanderboom et al., 2021). It may be that the differences are due to a greater incorporation of multiple muscle groups and as such higher demands on VO_2 with running compared to cycling at a given exercise intensity (Gleser, Horstman & Mello, 1974; Reybrouck et al., 1975), resulting in a slower clearance of circulating sEVs. Although, whether running elicits greater VO_2 demands in comparison to cycling is controversial (Millet, Vleck and Bentley, 2009) and thus, this remains as speculation.

1.6) Functional role of sEVs in tissue crosstalk during exercise

It was first addressed by Whitham et al., (2018), through their proteomic analysis, that significantly upregulated sEVs during exercise cargoed proteins associated with a broad array of biological functions including signal transduction, regulation of immune cell proliferation, leukocyte cell adhesion, integrin mediated signaling, glycolysis, and carbohydrate catabolism. Notably, of the 12 proteins identified that were associated with glycolysis, 6 significantly increased in isolated sEVs with exercise. Further analysis via the SignalP server (Petersen et al., 2011) revealed that none contained a signal peptide, suggesting that the proteins were secreted by non-classical secretion, in sEVs. In support of this, it has been shown that when exposed to glucose starvation cardiomyocytes upregulate the packaging of proteins and miRNA associated with metabolic processes such as glycolysis, gluconeogenesis, and pyruvate metabolism as well as signaling pathways involved in MAPK signaling and oxidative phosphorylation (Garcia et al., 2015). Furthermore, co-culturing H9C2 (immortalized cardiomyocytes) cells expressing CD63 with a GFP tag (CD63-GFP) from both glucose and non-glucose starved conditions with endothelial cells revealed significant

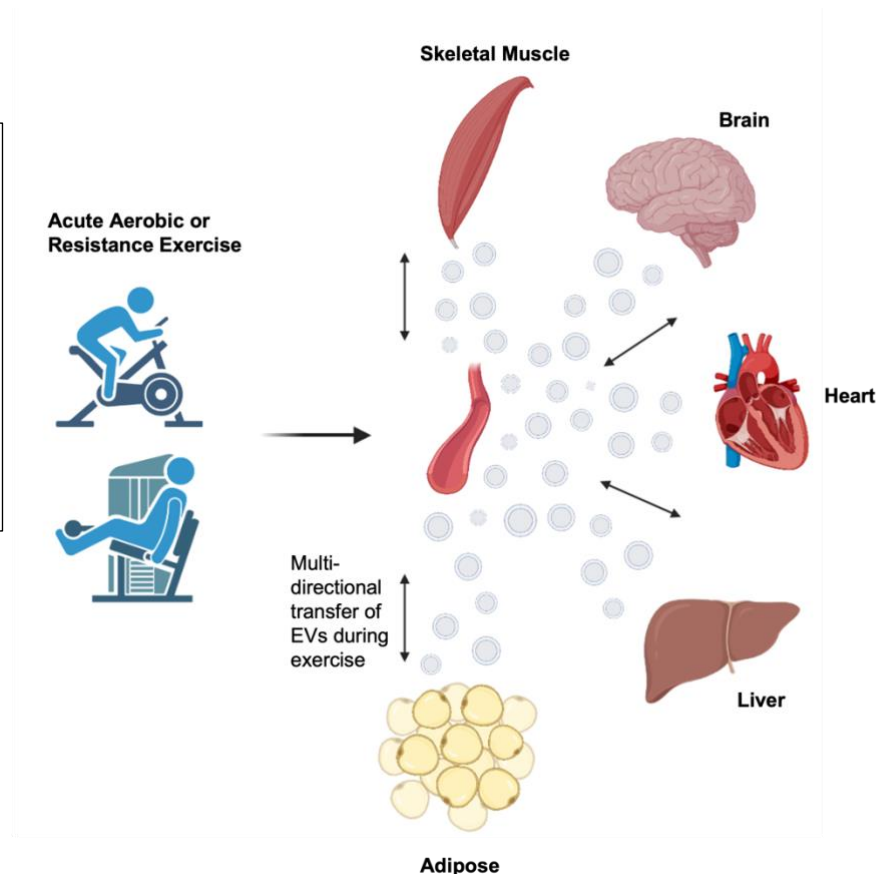
uptake of CD63-GFP exosomes into endothelial cells. Due to their anatomical proximity, the authors insinuate that exosomal transfer of proteins and miRNAs between cardiomyocytes and endothelial cells is a method by which metabolic homeostasis during glucose starvation can be regulated between the two cell types *in vivo* (Garcia et al., 2015). Which is an interesting concept, seeing as high intensity exercise is already known to mediate myocardial glucose uptake by interactions with endothelial produced nitric oxide synthase (Tada et al., 2000; Kemppainen et al., 2002).

To evaluate the tropism of exercise derived sEVs, Whitham et al., (2018) injected resting mice with labelled sEVs (lipophilic carbocyanine DiOC18 DiR) isolated from the plasma of both sedentary and exercise donor mice. From this, whole-body intravital fluorescent imaging showed that exercise derived sEVs are more readily taken up by the liver (Whitham et al., 2018). Significant increases in the incorporation of adhesion molecules, including integrin beta 5 (ITGB5), a membranous protein involved in vesicle adhesion, into sEVs with exercise, led to the hypothesis that changes in EV protein signature, may be involved in directing EVs to the liver (Whitham et al., 2018). Similar results have been observed in resting mice subject to tail-vein injection of sEVs labelled with DiR lipophilic dye. 24 hours after the injection, the authors reported incorporation of labelled sEVs into multiple tissues around the body including, the liver, spleen, lungs, heart, brain, pancreas, GI-tract, and quadriceps (Aswad et al., 2014). Although, it has been previously reported that the route of *in vivo* administration (i.e., intravenous, intraperitoneal, subcutaneous) of sEVs into mice does influence their biodistribution to tissues around the body (Wiklander et al., 2015), the fact that injection of sEVs at the same concentration from

sedentary and exercise conditions behaved in different manners through the same route of administration suggests that exercise influences EV protein signature which has the potential to direct EV tropism (Whitham et al., 2018).

sEVs contribute to tissue crosstalk during exercise through the release and uptake of exercise derived sEVs, as shown in Figure 2. These sEVs have the potential to transfer cargo that may regulate cellular metabolism, as well as a broad array of other biological functions (Whitham et al., 2018). Recent work has contributed to unravelling the capacity for exercise sEVs to positively regulate cardiac, adipose, and liver in the mitigation of T2DM and CVD, through changes in protein and miRNA profiles promoting reductions in myocardial apoptosis and necrosis in cardio-protection (Bei et al., 2017), as well as the browning of white adipose tissue (Oliveira et al., 2018; Di et al., 2020) and improvements in hepatic glucose and insulin tolerance (Castano et al., 2020). Furthermore, research has investigated the positive involvement of exercise sEVs in healthy aging as well as age-related cognitive decline (Bertoldi et al., 2018), Alzheimer's disease (Fuller et al., 2020), angiogenesis and endothelial function (Ma et al., 2018), pro-oxidant, antioxidant, and ROS regulation (Bodega et al., 2019). Moreover, sEVs derived from exercise have been implemented in many other health benefits by linking physiological outcomes with changes in circulating sEV protein and miRNA cargo (i.e., increases or reductions in circulating sEV miRNA content) (Trovato et al., 2019; Denham & Spencer, 2020; Vechetti et al., 2021; Siqueira, Palazzo & Cechinel, 2021). Although, attributing biological alterations merely through changes in protein and miRNA content alone, without showing a clear effect of EV cargo on a desired outcome, has its obvious limitations. Therefore, many of these processes require further research to understand their full potential in exercise adaptation.

Figure 2. Circulating EVs in multi-tissue crosstalk during exercise. Exercise causes the rapid secretion of EVs into the circulation from multiple cells and tissues around the body, which have the potential to contribute to tissue crosstalk through the transfer of luminal cargo.



1.7) Skeletal muscle derived sEVs

The role of exercise sEVs on the mitigation of obesity, CVD and T2DM has drawn a lot of attention to the regulation of adipose, liver, and skeletal muscle tissue crosstalk. However, little is understood about skeletal muscles contribution to this adaptive response. It has become evident that muscle cells are capable of secreting sEVs into the extracellular space (Guescini et al., 2010; Le Bihan et al., 2012; Romancino et al., 2013; Forterre et al., 2014), with the capability of packaging muscle enriched proteins and miRNAs (termed myomiRs) (Forterre et al., 2014; Mytidou et al., 2021). Forterre et al., (2014) identified significantly different protein compositions of sEVs derived from the mouse murine muscle cells C2C12 at myoblast or differentiated to myotubes. Notably, C2C12 myoblast sEVs treated with myotube sEVs induced early cellular differentiation of myoblasts to myotubes, suggesting that sEVs might be involved in

the early development of skeletal muscle (Forterre et al., 2014). Similarly, other groups have provided evidence for local skeletal muscle crosstalk (Estrada et al., 2021; Mytidou et al., 2021). One hypothesis being that skeletal muscle can regulate local homeostasis via the transfer of sEVs which are involved in muscle damage and repair through proper assistance in pro-inflammation, extracellular matrix (ECM) turnover, and satellite cell proliferation and differentiation down the myogenic pathway (Bittel & Jaiswal, 2019). Seeing as skeletal muscle is made up of multiple different cell types, it is comprehensible that sEVs are transferred locally as a method of crosstalk to regulate muscle dynamics (Estrada et al., 2021; Mytidou et al., 2021).

In a study by Castano et al., (2020) it was shown that chronic exercise can modulate circulating sEV bound miRNA content through the upregulation of miR-133a, -133b and -206 after a 5-week high intensity exercise program, in mice (Castano et al., 2020). Notably, a 4-week injection of exercise derived sEVs isolated from the skeletal muscle interstitial fluid into sedentary mice exerted significant improvements in glucose tolerance in comparison to sEVs isolated from liver under the same conditions. The authors propose that due to the enrichment of myomiRs miR-133a, -133b and -206 in skeletal muscle interstitial exosomes and the proximity of their isolation to the tissue, that these exosomes were derived from skeletal muscle. Furthermore, transfection of a miR-133b mimic onto primary hepatocytes reproduced similar improvements in glucose and insulin tolerance as plasma derived sEVs from exercising mice. Through the similar action of Foxo1 knockdown and the transfection of miR-133b, it is suggested that skeletal muscle sEVs modulate improvements on hepatic glucose tolerance and insulin sensitivity through transfer of miR-133b downregulating hepatic Foxo1 (Castano et al., 2020), in response to chronic exercise, *in vivo*.

As such, exercise may influence tropism of skeletal muscle sEVs to the liver (Whitham et al., 2018), by which they can regulate improvements in hepatic glucose and insulin tolerance (Castano et al., 2020). However, a major limitation in concluding the functional role of skeletal muscle sEVs in crosstalk is restricted by the ability to clearly identify skeletal muscle EV secretion into the circulation. As such, whether they contribute to the circulating exercise secretome is not known.

1.8) The relevance of protein markers in tissue specific EV detection

The use of protein markers to separate EV populations provides a method of overcoming difficulties in the separation of tissue specificity. The protein packaging into EVs is altered under different stimuli (van der Vlist et al., 2012). The recognition of these changes between various tissue allows EV subpopulations to be established by origin. Detecting and isolating EVs based on specific protein markers overcomes many limitations with co-isolating unwanted aggregates and vesicle bound entities as the need for prior purification steps is reduced. To date, current knowledge of protein markers that allows for the clear separation of skeletal muscle derived EVs from other cell types is limited. Guescini et al. (2015) highlighted that miR-206 coeluted at densities corresponding to sEV fractions (1.11g/ml) isolated from human plasma, suggestive of skeletal muscle sEV release into the circulation. The authors showed by immunoblotting and PCR that miR-206 co-localized in alpha-sarcoglycan (SGCA) positive sEVs, which were also confirmed by the expression canonical sEV markers CD81 and TSG101. Similarly, Brahmere et al., (2019) suggested that skeletal muscle sEVs contribute minimally to the circulation due to the lack of SGCA+sEV detection in exercise plasma by immunoblotting. However, this was contradicted by Rigamonti et

al., (2019) who identified an increase in circulating SGCA+sEVs with acute exercise by the same methods. The sarcoglycan complex, consisting of α , β , γ and δ subunits, is a highly abundant protein in human and rat skeletal muscle that interacts with dystrophin-associated glycoprotein complex (DGC), involved in sarcolemma stabilization and signal transduction to anchor the sarcolemma and extracellular matrix during muscle contraction (Tarakci & Berger, 2016). The gene SGCA has been found to be strictly expressed in striated skeletal muscle (Liu & Engvall, 1999). Thus, the authors propose that the co-detection of SGCA alongside CD81 in systemic sEVs is somewhat indicative of a skeletal muscle sEV secretion into the circulation (Guescini et al., 2015). However, the abundance of a protein in a tissue does not translate to EV specificity. More so, the reliability of CD81 as a canonical exosome marker has been questioned (Kugeratski et al., 2021). Interestingly, proteomic profiling of the mouse murine immortalized muscle cell line, C2C12, indicated that secreted sEVs from the muscle contained >400 proteins (Forterre et al., 2015) of which 22 other proposed muscle specific proteins were identified. Therefore, as to whether SGCA accounts for all muscle derived EVs is unclear.

1.9) The use of global proteomics in skeletal muscle EV protein marker discovery

Previous studies that have attempted to address skeletal muscle EV protein markers through the evaluation of a small number of proteins via target methodologies (Guescini et al., 2015; Brahmere et al., 2019; Rigamonti et al., 2019), without the prerequisite of global analysis, are limited by coverage and comparison. Therefore, the use of non-bias, high discovery methodological approaches for protein identification to separate different EV populations is crucial for effective isolation and

detection. In recent years, the adoption of mass spectrometry-based proteomics as a method of protein marker discovery has gained attention through the ability to detect thousands of proteins within various biological environments (He & Chiu, 2003; Veenstra et al., 2007; Good et al., 2007; Tambor et al., 2009; Lisitsa et al., 2014). The mass gathering of proteomic data from human tissues and cells makes up the human protein atlas; an understanding of the enrichment of proteins across all tissues around the body (Uhlen et al., 2015). The human genome is proposed to express 20,000 – 25,000 open reading frames, by which DNA can be transcribed into amino acid sequences. With the potential of all proteins to be modified post-transcriptionally or post-translationally, a single human sample could contain upwards of 100,000 different protein species (Veenstra et al., 2007). Similarly, the adoption of global proteomic based analysis offers a method of overcoming the many limitations in plasma biomarker discovery (Geyer et al., 2017). Notably, one that can allow for the unravelling of the circulating EV proteome. As EV proteomic research progresses, providing a more comprehensive understanding of the EV proteome between cells, tissues and biofluids as well as the influence of different stimuli on protein phenotype; a better understanding of protein marker specificity will arise. Much like the culmination of various studies that have contributed to vesicle specific databases such as VesiclePedia (Kalra et al., 2012) and ExoCarta (Keerthikumar et al., 2016) for the classification of vesicle bound proteins. Examples already exist of the adoption of proteomics in the classification of putative exosomal markers (Kugeratski et al., 2021), skeletal muscle C2C12 myotube derived sEVs (Forterre et al., 2015), and changes in the circulating sEV proteome with exercise (Whitham et al., 2018; Vanderboom et al., 2021; Kobayashi et al., 2021). However, data concerning skeletal muscle derived EV

markers *in vitro* and *in vivo* with exercise, through the utilization of proteomic data coupled with targeted methods, is limited.

With this in mind, the aim of the present study was to identify novel candidate protein markers of skeletal muscle sEV secretion in humans *in vivo*. Initially, the present study curated, re-analyzed and overlaid several online proteomic datasets as a hypothesis generating model to inform protein marker identification of skeletal muscle derived sEVs. Next, the aim was to evaluate the specificity of the candidate protein markers to muscle sEVs by analyzing and comparing protein expression amongst isolated sEVs from C2C12 myotube against several human cell lines. Moreover, *in vitro* models of exercise and muscular contraction including electrical pulse stimulation (EPS) and calcium influx by ionomycin (IM) were applied to determine the extent to which the candidate markers were exercise responsive *in vitro*. Finally, a high intensity interval exercise (HIIE) protocol was employed, by which plasma sEVs were isolated and analyzed pre and post exercise using ExoView and immunoblotting to fully evaluate how these protein markers translated *in vivo* and in line with the original hypothesis produced by the proteomic analysis.

2. Materials and Methods







A list of all antibody details as well as cell lines, reagents and resources used within the present study have been described in Table 2 and Table 3, respectively. All media formulas have been noted in Table 4.

2.0) Proteomic analysis

Re-analysis of quantitative datasets regarding 24 hour EPS of human primary myotubes and arterial EV proteome post exercise: Firstly, the Laurens et al., (2020) dataset was selected for re-analysis. This proteomic dataset contained an analysis of the array of proteins released from C2C12 myotubes into conditioned media with EPS over (10V, 2ms-pulse, 0.1Hz) an acute (3 hours) or chronic (24 hours) setting and was utilized in the present study to observe changes in secreted proteins with an *in vitro* model of muscular contraction. Next, the Whitham et al., (2018) dataset which focused on analyzing the circulating EV proteome in human arterial plasma before and after 60 minutes exhaustive exercise was chosen to evaluate proteins that were contained within EVs and that were upregulated in exercise in human plasma. Together, both datasets were re-analyzed to evaluate significantly upregulated proteins secreted from muscle with stimulation and in plasma EVs post exercise. To do this, output files from MaxQuant for Laurens et al., (2020) (PXD014126) and Whitham et al., (2018) (PXD006501) were downloaded from the publicly available database PRIDE (Perez-Riverol et al., 2019). LFQ (label free quantitative) intensity regarding arterial EV exercise (Whitham et al., 2018) and 24 hour control and EPS (Laurens et al., 2020) data were extracted from the protein groups files and were analyzed by Perseus v1.6.15.0 (Tyanova et al., 2016). Prior to statistical analysis, proteins were filtered by (i) known modified sites, (ii) if they were recognized

contaminants, (iii) the presence of protein sequences matching artificially generated decoy sequences. Both Whitham et al., (2018) and Laurens et al., (2020) original analyses was more liberal as the focus was on larger scale protein detection, as such proteins were required to have 27.3% or $n = 3/11$, and 75% or $n = 3/4$ valid values amongst participants / replicates, respectively. However, to provide greater confidence in candidate protein marker discovery amongst multiple participants / replicates in the present re-analysis, a more conservative approach was adopted. As such, valid values were required to be present in 100% ($n = 4/4$) of replicates for the Laurens's EPS data and 70% ($n = 8/11$) of participants in the Whitham arterial exercise EV dataset. From this, data was grouped accordingly. For Laurens EPS data, groups consisted of 24 hour control and 24 hour EPS, for Whitham's arterial plasma EV data, groups contained rest and exercise. Regarding EPS, data was normalized to the median of the 'control' data and for arterial EV exercise, data was normalized to the median of 'pre' data. Both datasets were then Log^2 transformed. All data was normally distributed. Laurens EPS data was analyzed by an unpaired two samples t-test comparing control vs stimulated. For the Whitham arterial EV exercise data statistical analysis was performed using a paired two samples t-test comparing rest vs exercise. To note, the 3 hour time point for both control and stimulated conditions from the Laurens dataset were not regarded for further analysis due to a lack of change in protein expression seen at this time point. From this, only the 24 hour time point for both conditions was used in the proteomic overlay. For both datasets, statistical analysis considered $S0 = 0.1$ and permutation-based FDR correction = $P < 0.05$. Volcano plots were generated using Perseus v1.6.15.0.

Figure 3. Details of proteomic datasets and their inclusion in the Perseus overlay.

Study	Author	Original analysis	Quantitative data (re-analysis)	Non-quantitative (presence/absence)	Perseus overlay for matching gene names
	Laurens et al., 2020	Secreted proteins from human primary myotubes with and without EPS	<input checked="" type="checkbox"/>		<input checked="" type="checkbox"/>
	Whitham et al., 2018	Human arterial plasma EVs pre and post exercise	<input checked="" type="checkbox"/>		<input checked="" type="checkbox"/>
	Deshmukh et al., 2015	Mouse skeletal muscle proteome (basal)		<input checked="" type="checkbox"/>	<input checked="" type="checkbox"/>
	Forterre et al., 2014	C2C12 myotube sEVs (basal)		<input checked="" type="checkbox"/>	<input checked="" type="checkbox"/>
	Kalra et al., 2012	VesiclePedia compendium of EV proteins		<input checked="" type="checkbox"/>	<input checked="" type="checkbox"/>
	Keerthikumar et al., 2016	ExoCarta compendium of EV proteins		<input checked="" type="checkbox"/>	<input checked="" type="checkbox"/>

Proteomic overlay: Next, the aim was to filter for protein marker candidates based on presence vs absence using non-quantitative datasets. Significantly upregulated proteins from the re-analysis of Laurens et al., (2020) and Whitham et al., (2018) were cross referenced with proteins identified in 4 non-quantitative datasets obtained from extracting protein group files downloaded from PRIDE. Firstly, the Deshmukh et al., (2015) dataset regarding a deep proteomic analysis of mouse skeletal muscle proteome was used to identify highly abundant skeletal muscle proteins, to confirm that the candidate proteins markers detected are enriched in skeletal muscle. Next, to further ratify the presence of these proteins in muscle EVs, the Forterre et al., (2015) dataset, which involved an analysis of C2C12 myotube sEVs, was adopted. Finally, to address proteins already identified as components of EVs, proteins were cross references with the VesiclePedia (Kalra et al., 2012) and ExoCarta (Keerthikumar et al., 2016) databases. To cross reference similar proteins amongst datasets, all 6 (2

quantitative and 4 non-quantitative; see Figure 3) datasets were uploaded to the same matrices in Perseus. By using the 'matching row by gene name' functionality, which recognized matching UniProt Gene identifiers enabled filtering of proteins not commonly expressed amongst all 6 datasets. As such, the final overlay identified proteins that were common to all 6 datasets. An overview of this process is presented in Figure 3. A list of gene names for all 6 datasets were uploaded to <https://bioinformatics.psb.ugent.be/webtools/Venn/> to generate a Venn Diagram presenting a visual representation of which protein candidates were common to all.

2.1) Cell line protocol

Cell Culture: All cells were seeded at a density of 2 million cells per flask (T75) or dish (10cm). C2C12 myoblasts were seeded into 10cm dishes coated with 1mM Matrigel to improve myogenic differentiation and maturation (Langen et al., 2003; Balci & Dinçer, 2009; Denes et al., 2019) and decrease cellular death (Langen et al., 2003). All other cell lines were seeded into treated or non-treated T75 flasks, dependent on their adherence. For cellular growth, C2C12 myoblast, HEK293, Jurkat, Hela, SH-SY5Y and U2OS cells were cultured in DMEM growth media (Table 4). INS-1 cells were cultured in RPMI-1640 growth media (Table 4). All cells were grown to ~90% confluency before media or cell collection. To induce differentiation of C2C12 myoblasts to myotubes, C2C12 myoblasts were cultured in differentiation media (Table 4) after cells had reached ~90% confluency. Fresh differentiation media was applied every 24 hours for 7 days.

EV-depletion: Seeing as bovine serums contain considerable amounts of EVs (Shelke et al., 2014; Aswad, Jalabert and Rome, 2016) from which proteins and RNAs may interfere with the clarity of *in vitro* readouts for sEV analysis (Shelke et al., 2014; Wei et al., 2016; Aswad, Jalabert and Rome, 2016; Pavani et al., 2019; Lehrich et al.,

2021) both FBS and horse serum were subject to a 16hr overnight ultracentrifugation (UC) (S50-fixed angle rotor) at 110,000 x g at 4°C, using a Sorvall MTX 150 Micro-Ultracentrifuge (ThermoFisher Scientific, Leicestershire, UK) by which sEVs were pelleted and extracted. The remaining supernatant was then used to supplement media to generate EV-depleted growth or differentiation media. Prior to collection, non-differentiating cell lines were washed in PBS and placed in RPMI-1640 (INS-1) or DMEM (HEK293, Jurkat, Hela, SH-SY5Y, U2OS) EV-depleted growth media (Table 4), according to the cell line for 48 hours before the conditioned media was collected. For C2C12 myotubes, EV-depleted differentiation media (Table 4) was applied on day 7 of differentiation and left for 48 hours. Cell viability was assessed daily via the EVOS XL Core Imaging System (ThermoFisher Scientific Ltd, Leicestershire, UK) to determine the extent of cellular death (images for C2C12 growth and differentiation are shown in Figure S2). Using an Automated Cell Counter (ThermoFisher Scientific Ltd, Leicestershire, UK), EV-depleted cells were 100% viable prior to collection. All conditioned media was collected and stored in 50ml falcon tubes at -80°C prior to EV isolation. All cells were grown and maintained at 37°C in humidified air containing 5% CO₂.

2.2) *In vitro* stimulation of C2C12 myotubes

Electrical Pulse Stimulation (EPS): C2C12 myoblasts were seeded into 6 well plates at a density of 200,000 cells per well. Myoblasts were differentiated for 7 and 8 days, as described above. To generate the PRE time point, C2C12 myotubes were differentiated for 7 days, washed once in PBS, and changed to EV-depleted differentiation media before being left for 24 hours for EV production. Conditioned media was then collected and stored at -80°C. Both control and stimulatory conditions

were differentiated for 8 days, before being changed to EV-depleted differentiation media. At this point, electrodes were placed into the media and subject to either stimulation (STIM) or control (CTL) conditions. EPS was conducted using a C-PACE EP multichannel culture pacer (IonOptix, Milton, MA) and entailed a 2ms-pulse at 11.5V, with a frequency of 1Hz for 24 hours. Following 24 hours, media from both conditions was collected (0Post), cells were then washed in PBS and fresh EV-depleted differentiation media was applied. Both conditions were then left for a further 24 hours before media was collected (24Post). All media was stored immediately after collection in 50ml falcon tubes at -80°C, prior to EV isolation. To examine the effect of EPS on cellular signaling pathways activated by muscular contraction at different time points, cells were lysed before (PRE), immediately after (0 h), 3hours after (3 h), and 24 hours post (24 h). C2C12 myotubes were washed once in ice cold PBS and then lysed over ice using 500µl of 1 x RIPA-Buffer and stored in 1.5ml Eppendorf's at -80°C.

Ionomycin (IM): Differentiation of C2C12 myoblasts to myotubes was the same as previously described. On day 7 of differentiation C2C12 myotubes were placed in EV-depleted media supplemented with IM (1µM + 99.8% ethanol) or the vehicle control (CTL) consisting solely of ethanol (ETOH, 99.9%). After 24 hours (Day 8), the conditioned media was collected in 50ml falcon tubes and stored at -80°C ready for EV isolation. To determine cell viability and the effects of the treatment on myotube structure, images were taken daily from the start of differentiation (Day 0), prior to IM treatment (Day 7) and post treatment prior to collection (Day 8), using the EVOS XL Core Imaging System (ThermoFisher Scientific Ltd, Leicestershire, UK).

2.3) High Intensity Interval Exercise (HIE)

Participant recruitment: A total of five participants were recruited for this study (Table 1). The participants were healthy (as defined by the Department of Health General Practice Physical Activity Questionnaire 2006) without any previous history of cardiovascular, respiratory, metabolic, or neurological disease. All practices were performed in line with the Declaration of Helsinki. Each participant gave signed, informed consent, and completed the full exercise program. Ethics were approved by the University of Birmingham Ethics Committee (ethical approval number ERN_17-1570).

Table 1. Subject details

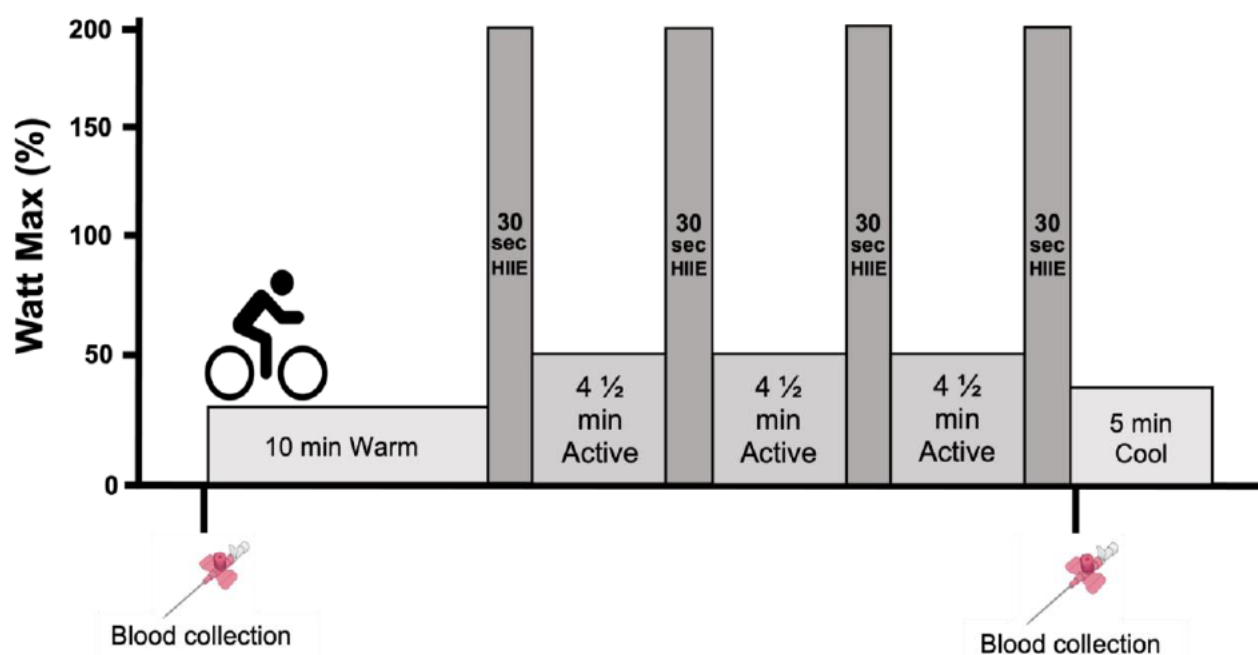
Exercise Participants	Participant details		
	Gender	Age	VO ₂ max (L/kg/min)
	Male (n=2) Female (n=3)	22±5.2	42.88±4.4

Values = Mean ± SD

Testing and Exercise Protocol: Participants were required to refrain from consuming caffeine < 6 hours, a large meal < 4 hours and a light snack < 2 hours prior to each exercise session including the testing session. Participants were required to attend an initial exercise testing session, followed by one HIE session providing at least 48 hours between sessions but no longer than 2 weeks. Participants were advised to drink 0.5 liters of water within 4 hours and a further 0.25 liters within 15 minutes of testing to insure adequate hydration. Exercise testing consisted of a standardized incremental aerobic cycling protocol consisting of a 5 minute warm-up at 50W prior to a ramped protocol by which loaded resistance increased every 3 minutes until participants reached volitional exhaustion, followed by a 2 minute cool down. Oxygen

consumption was measured through a mask attached to a Vyntus Metabolic Cart. Heart rate and power output were also measured. The participants subsequent VO_2 max and Watt max (W_{max}) were calculated from this. The participants W_{max} were used to define the subsequent exercise session intensities. For the HIIE protocol (displayed in Figure 4), a 10 minute warm up at a light-moderated intensity was conducted, followed by 4 x 30 seconds all out cycling at 200% W_{max} , with 4 ½ minutes of active recovery between sets at 50W. Participants then completed a 5 minute light cool down resulting in 35 minutes total exercise duration.

Figure 4. High intensity interval exercise (HIIE) protocol



Blood Collection: Blood analysis was performed on each participant during a singular 200% W_{max} session. Blood samples were treated identically pre- and post-exercise protocol. A cannula was inserted into a vein within the cubital fossa prior to the exercise bout. In each case, the cannula was infused with saline and allowed to adjust for ~2 minutes. In both conditions, 2ml of venous blood was sampled and disposed of to clear any contamination due to damage to cell linings. Then, 5 x 10ml blood samples

were collected pre-, at 10 minutes supine resting and post-, within 30s cessation of the exercise protocol, in EDTA lined tubes (Figure 4).

Platelet Free Plasma (PFP): Platelets continue to secrete EVs after blood collection and therefore can be a major source of contamination (Bæk et al., 2016). Therefore, to generate PFP, blood samples were exposed to a 2 x centrifugation protocol within 2 minutes of sampling. Samples were initially spun at 2500 x g for 15 mins at room temperature. Plasma was removed leaving a ½ cm before the buffy coat to avoid contamination and placed in separate tubes. Plasma was then spun again at 2500 x g for 15 minutes at room temperature to achieve PFP. PFP samples were stored at -80°C prior to EV isolations.

2.4) Isolation of sEVs

Ultracentrifugation (UC): Human PFP samples and conditioned media were subject to an overnight thaw at 4°C. Conditioned media was centrifuged at 400 x g at room temperature for 10 minutes and then again at 2000 x g for 20 minutes at 4°C to clear cellular debris and pellet larger vesicles, respectively, using a Sorvall Legend X1 centrifuge (ThermoFisher Scientific, Leicestershire, UK). The supernatant was then removed, leaving the pellet intact, and spun at 110,000 x g for 2 hours at 4°C using a S50-A fixed angle rotor inside a Sorvall MTX 150 Micro-Ultracentrifuge, to pellet smaller vesicles. The supernatant was then removed, and the EV pellets were resuspended in 1.5ml PBS and transferred to 1.5ml micro-ultracentrifuge tubes and spun again in a S55-A2 fixed angle rotor at 110,000 x g for 2 hours at 4°C to pellet sEVs. For sEV isolation from PFP samples, once thawed, samples were subject to the same UC protocol as described. Non-EV fractions were taken from the conditioned media after the first 2 hour UC cycle and used as a comparator for sEV protein

analysis. After the second UC cycle, the PBS was removed being careful to leave the pellet intact and the sEV pellets were lysed in 1 x Tris-SDS buffer (20mM Tris-HCl; 2% (w/w) SDS). Non-EV fractions were lysed in 5 x Tris-SDS buffer (100mM Tris-HCl; 10% (w/w) SDS). sEV pellets from conditioned media and human plasma were then sonicated using a Bioruptor Plus Sonication System (Diagenode, Leige, Belgium) for 6 x 30 seconds at 4°C to degrade the EV membrane and improve solubilization of all EV proteins ready for analysis. All samples were then stored at -80°C.

Size Exclusion Chromatography (SEC): C2C12 conditioned media was subject to an overnight thaw at 4°C. To remove cellular debris and larger particles, and to increase the concentration of EVs in thawed media, conditioned media was placed in Amicon Ultra-15 filters (Merck Life Science, Darmstadt, Germany) and subject to centrifugation at 4000 x g for 10 minutes at room temperature producing 5ml concentrated conditioned media. The 5ml conditioned media was loaded into a qEV10 column (Izon, Oxford, UK) containing agarose resin, used to separate particles based on size. The Automated Fraction Collector (Izon, Oxford, UK) enabled the separation and collection of 7 fractions of 500µl each. According to manufacturing guidelines, fractions 1-3 contain sEVs, whereas fractions 4-7 contain non-vesicle components. To increase protein yield from each fraction, fractions were further concentrated by centrifugation at 4000 x g for 30 mins at room temperature in Amicon filters. The resulting solutions were placed in 1.5ml eppendorfs and lysed in 50µl of 5 x Tris-SDS buffer, before being subject to sonication (see UC protocol above for details) to improve protein solubility, before being stored at -80°C.

Immunomagnetic Precipitation (IMP): IMP isolation was conducted through the EasySep™ Human Pan-Extracellular Vesicle Positive Selection Kit and EasySep™ magnet (StemCell Technologies, Vancouver, Canada). According to manufacturing

guidelines, 6ml of plasma or conditioned media was incubated in a Selection Antibody Cocktail Mix containing anti-CD9, anti-CD63 and anti-CD81 for 10 minutes at room temperature, followed by the addition of the magnetic Releasable RapidSpheres, which were incubated with the sample for a further 10 minutes at room temperature to allow the attachment of magnetic spheres to CD9, CD63 and CD81 antibodies previously used in the cocktail. Sample was topped up to 10ml using D-PBS (without calcium or magnesium) before the tube was placed in the magnet and left for 5 minutes at room temperature. After 5 minutes, the supernatant at the bottom of tube was discarded and the sample was flushed 3 times with D-PBS. After removing the tube from the magnet, the remaining sample contained sEVs bound by CD9, CD63 and CD81 antibodies. To separate the RapidSpheres from the isolated sEVs, the sample was treated with 1 x Tris-SDS buffer and subject to centrifugation at 5000 x g for 5 minutes at room temperature from which the supernatant containing the sEVs was extracted. Finally, the sample was sonicated (see UC protocol above for details) to improve protein solubility and stored at -80°C.

2.5) Sample preparation and Immunoblotting

Sample Preparation: Lysates from plasma sEVs and cell derived sEVs were thawed on ice. Total protein content of each sample was measured using the DC (detergent compatible) colorimetric protein assay. Samples were diluted in ddH₂O and compared to a standard curve generated by BSA (bovine serum albumin) protein standards in a 98-well plate read out by a multi-mode microplate reader (BMG Labtech, Offenburg, Germany). Samples were prepared at the same protein concentrations ($\mu\text{g}/\mu\text{l}$) in 1 x NuPAGE LSD sample buffer containing BME (2-mercaptoethanol) and left overnight at room temperature. Samples were stored at -80°C prior to analysis.

Immunoblotting: Samples were normalized to total protein ($\mu\text{g}/\mu\text{l}$) and subject to SDS-PAGE (sodium dodecyl sulfate-polyacrylamide gel electrophoresis) using homemade Bis-Tris gels (10%) in 1 x MOPS SDS running buffer for 10 minutes at 100V and then 50 minutes at 150V. Proteins were then transferred onto 2% PVDF (polyvinylidene difluoride) membranes in 1 x Transfer Buffer (48mM Tris-HCl; 39mM glycine; 10% (v/v) methanol) for 60 minutes at 100V. Membranes were placed in blocking solution (5% Milk powdered in TBS-T; Tris-buffered Saline Tween-20) for 60 minutes. Membranes were incubated at 4°C with corresponding primary antibodies (Table 2) and left overnight. Membranes were washed in TBS-T for 3 x 5 minutes to remove primary antibody and then incubated in secondary antibody (Table 2) for 60 minutes at room temperature. Membranes were washed again for 3 x 5 minutes to remove secondary antibody and placed in ECL (electrochemiluminescence) for 2 minutes prior to imaging. Imaging was conducted using a G:BOX Chemi-XR5 using GeneSys software (SynGene, Cambridgeshire, UK). Images were quantified using ImageJ software.

2.6) Nanoparticle Tracking Analysis (NTA)

EV size and concentration was determined using Nanosight LM10 instrument (Malvern Instruments, Amesbury, UK) equipped with a red laser (638 nm). The analysis was performed by the same user to minimize variability in the measurement. EVs isolated via UC (1 x 110,00g) from 50ml of conditioned media were resuspended in 1ml of particle-free PBS and passed through a 20 μg needle to reduce aggregation. A 50 μl aliquot of the sample was taken and stored at -80°C for later analysis. Upon thawing, samples were then diluted in particle-free PBS to a final volume of 1ml at a 1:100 dilution. All videos were processed using NTA 3.3 build 3.3.104 software (Nanosight

Ltd.) and six consecutive 60-second recordings were made for each sample with a total of 1800 frames per measurement. The following settings were used; camera level 15, viscosity 1 (for PBS), detection threshold 6 and all other parameters were set at default. Samples were injected manually and advanced when promoted between videos.

2.7) ExoView

Samples were analyzed using the Exoview® R100 (NanoView, Biosciences, Boston, MA, USA). Analysis was performed in accordance with manufacturing guidelines. (<https://www.nanoviewbio.com/exoview-r100>). Briefly, the dilution of samples consisted of a 1:100 serial dilution of plasma to incubation solution. Chips were removed from storage at 4°C and left to adjust to room temperature. The chips were then placed in individual wells leaving the antibody coated center containing capture spots for anti-CD9, anti-CD63, anti-CD81 and Mouse IgG face up (Table 2). 35µl of incubated plasma sample was added onto each of the chips and covered with foil to prevent UV (ultraviolet) penetration and incubated at room temperature for 16 hours. The chips were then washed in wash solution and shaken on a microplate shaker at 500rpm for 3 minutes. 750µl solution was removed from the chips and they were washed once more in wash solution. Chips were incubated for an hour in the dark at room temperature with the fluorescently labelled ExoView Tetraspanin Cargo Kit (CD9 blue; CD63 red; CD81 green) for 60 minutes which was preprepared prior to incubation in blocking solution (CD9 1:500; CD63 1:500; CD81 1:500) (Table 2). The chips were then washed 3 x in wash solution and carefully transferred to a 10cm dish containing rinse solution. Once rinsed, chips were then left to dry on absorbent paper and then placed in the ExoView reader for analysis. Data analysis was performed using

NanoView Analysis Program. Quantification was performed to calculate fluorescent counts based on the total number of vesicles individually expressing green (CD9), blue (CD63) and red (CD81) fluorescence present on each capture spot (i.e., total CD9 expression = counts of CD9 bound to CD9, CD9 bound to CD63 and CD9 bound to CD81) including analysis for background fluorescence (mouse IgG). Each chip was tested to get a background level prior to the incubation procedure. The data was then normalized based on the recorded background noise produced for each chip yielding a normalized count for vesicles.

2.8) Statistical analysis

Statistical analysis of proteomic data was performed using Perseus v1.6.15.0 and has been detailed above. Immunoblots were quantified using ImageJ and statistics were performed using GraphPad Prism version 9.3.0. A one-way ANOVA was employed to determine significant differences between protein expression amongst sEVs isolated from the several different cell lines. Bonferroni's post hoc test was used to identify where significant differences lay between and within groups. A two-way ANOVA was used to determine significant differences with EPS. For EPS, Bonferroni's post hoc test was used to test significant group-time interactions. Differences in IM vs CTL were analyzed using an unpaired two-tailed t-test. Statistical significance of pre and post exercise EV protein markers was analyzed using a paired two-tailed t-test. Differences were considered statistically significant at $P < 0.05^*$. All data has been plotted with individual data points, with the mean \pm SD. Quantification of cell lines is displayed as differences in protein expression. IM vs CTL data has been expressed as difference in fold change relative to the CTL. EPS and exercise data has been expressed as difference in fold change relative to the PRE of each group.

Table 2. Antibody Details

Antibody	Dilution	Source	Manufacturer	Catalogue no. (#)
Immunoblotting				
CD9	1:1000	Rabbit	Abcam	#ab92726
Syntenin-1	1:1000	Rabbit	Abcam	#ab19903
ALIX	1:1000	Rabbit	Abcam	#ab186429
TSG101	1:1000	Rabbit	Abcam	#ab125011
ANXA6	1:5000	Rabbit	Abcam	#ab226410
CD44	1:1000	Rabbit	CST	#37259
SGCA	1:1000	Rabbit	Abcam	#ab189254
Anti-rabbit IgG	1:1000	Goat	CST	#7074
ExoView				
ExoView Tetraspanin Cargo Kit	Nanoview Biosciences			
CD9	1:500			
CD63	1:500			
CD81	1:500			
Mouse IgG	1:500			
Negative Control				

Table 3. Reagents and Resources Details

Reagent or Resource	Supplier	Identifier / URL
Cell Lines		
C2C12 Myoblasts	American Type Culture Collection	CRL-1772
HEK293	American Type Culture Collection	CRL-1573

Jurkat	American Type Culture Collection	TIB-152
HeLa	American Type Culture Collection	CRM-CCL-2
SH-SY5Y	American Type Culture Collection	CRL-2266
U2OS	American Type Culture Collection	HTB-96
INS-1	Sigma-Aldrich	SCC207
Cell Culture		
T75 Tissue Culture Treated Flasks	VWR Collection	734-2313
T75 Non-Treated Flasks	ThermoFisher Scientific Ltd	156800
10cm Culture Treated Dishes	Scientific Laboratory Supplies	G664160
Matrigel	ThermoFisher Scientific Ltd	11573560
DMEM + 2mM L-glutamine	ThermoFisher Scientific Ltd	11520416
RPMI-1640 + 2mM L-glutamine	ThermoFisher Scientific Ltd	11875093
HEPES	ThermoFisher Scientific Ltd	15630106
GluteMax	ThermoFisher Scientific Ltd	35050061
Glucose	Merck Life Sciences Ltd	G7528
Sodium Pyruvate	Merck Life Sciences Ltd	S8636
Heat Inactivated Fetal Bovine Serum	Merck Life Sciences Ltd	F9665
Penicillin-streptomycin	ThermoFisher Scientific Ltd	11528876
Heat Inactivated Horse Serum	ThermoFisher Scientific Ltd	10368902
Ethanol	ThermoFisher Scientific Ltd	10000652

RIPA buffer	Scientific Laboratory Supplies	20-188
Automated Cell Counter	ThermoFisher Scientific Ltd	AMQAF1000
EVOS XL Core Imaging System	ThermoFisher Scientific Ltd	AMEX1000
<i>Electrical Pulse Stimulation (EPS) and Ionomycin (IM) C2C12 activation</i>		
C-PACE EP multichannel culture pacer	IonOptix	http://www.ionoptix.com/wp-content/uploads/2014/07/CPaceEP.pdf
6-well C-Dish	IonOptix	3516
Ionomycin, Calcium Salt	ThermoFisher Scientific Ltd	I24222
<i>High Intensity Interval Exercise</i>		
Lode Cycle Ergometer	Lode	960900
Vyntus™ CPX Breath by Breath Metabolic Cart	Vyaire Medical	
Cannula	Becton Dickinson	391452
EDTA Tubes	Becton Dickinson	VS367838
<i>Extracellular Vesicle Isolation</i>		
Sorvall Legend X1 Centrifuge Series	ThermoFisher Scientific Ltd	10036894
Sorvall MTX 150 Micro-Ultracentrifuge	ThermoFisher Scientific Ltd	46960
S50-A fixed angle rotor	ThermoFisher Scientific Ltd	45540
S55-A2 fixed angle rotor	ThermoFisher Scientific Ltd	45865
PBS	ThermoFisher Scientific Ltd	12549079
SDS	VWR International	A1112.0500
Tris-HCl	ThermoFisher Scientific Ltd	10724344
Bioruptor Plus Sonicator System	Diagenode	B01020001

qEV Automatic Fraction Collector	IZON	https://store.izon.com/products/automatic-fraction-collector-afc
Amicon Ultra-15 Centrifuge Filter Units	Merck Life Sciences	UFC910024
qEV10 / 70nm	IZON	SP3
NaOH	Merck Life Sciences	655104
EasySep™ Human Pan-Extracellular Vesicle Positive Selection Kit	StemCell Technologies	17891
EasySep™ Magnet	StemCell Technologies	18001
D-PBS (without calcium and magnesium)	StemCell Technologies	37350
ExoView® R100	NanoView Biosciences	
ExoView® Tetraspanin Cargo Kit	NanoView Biosciences	

Sample Preparation and Western Blot

DC Assay	Bio-Rad Laboratories Ltd	5000111
BSA	Fisher Scientific Ltd	12881630
FLUOstar Omega filter-based multi-mode microplate reader	BMG Labtech	
1x NuPAGE LDS	ThermoFisher Scientific Ltd	11559166
2-mercaptoethanol	ThermoFisher Scientific Ltd	10306050
Bis-Tris	VWR International	6976-37-0
40% Acrylamide	ThermoFisher Scientific Ltd	10001313
TEMED	Merck Life Sciences	T7024

APS	Merck Life Sciences	A3678
MOPS-SDS Running Buffer	ThermoFisher Scientific Ltd	NP0001
Glycine	VWR International	A1067.5000
Tween	VWR International	9005-64-5
NaCl	ThermoFisher Scientific Ltd	746398
Methanol	ThermoFisher Scientific Ltd	11976961
PVDF Membrane	Scientific Laboratory Supplies	10600021
ECL	ThermoFisher Scientific Ltd	11556345
G Box Chemi XR5	SynGene	
GeneSys Software	SynGene	
Image J	Image Processing and Analysis in Java	https://imagej.nih.gov/ij/
Nanoparticle Tracking Analysis (NTA)		
Nanosight LM10	Malvern Instruments	
NTA 3.3 build 3.3.104 software	Malvern Instruments	https://www.malvernpanalytical.com/en/support/product-support/software/nanosight-nta-software-update-v3-3
Statistical Analysis		
GraphPad Prism version 9.3.0	Prism	https://www.graphpad.com/scientific-software/prism/
Perseus version 1.6.15.0	MaxQuant	https://maxquant.net/perseus/

Table 4. Media Formulas

Media	Formula
Growth media (DMEM)	DMEM + 2mM L-glutamine supplemented with 5mM glucose, 10% heat inactivated fetal bovine serum (FBS), 100ul/ml penicillin, 100ug/ml streptomycin, 1mM sodium pyruvate and 1x GluteMax.
Growth media (RPMI-1640)	RPMI-1640 + 2mM L-glutamine supplemented with 11mM Glucose, 10mM HEPES, 10% heat inactivated fetal bovine serum (FBS), 50ul/ml penicillin, 50ug/ul streptomycin and 1mM sodium pyruvate.
C2C12 Differentiation media	DMEM + 2mM L-glutamine supplemented with 5mM glucose, 2% Horse Serum, 100ul/ml penicillin 100ug/ml streptomycin, 1mM sodium pyruvate and 1x GluteMax.
<i>EV-depleted media</i>	
EV-depleted Growth Media (DMEM)	DMEM + 2mM L-glutamine supplemented with 5mM glucose, 10% heat inactivated EV-depleted fetal bovine serum (FBS) , 100ul/ml penicillin, 100ug/ml streptomycin, 1mM sodium pyruvate and 1x GluteMax.
EV-depleted Growth media (RPMI-1640)	RPMI-1640 + 2mM L-glutamine supplemented with 11mM Glucose, 10mM HEPES, 10% heat inactivated EV-depleted fetal bovine serum (FBS) , 50ul/ml penicillin, 50ug/ul streptomycin and 1mM sodium pyruvate.
EV-depleted Differentiation media	DMEM + 2mM L-glutamine supplemented with 5mM glucose, 2% EV-depleted Horse Serum , 100ul/ml penicillin 100ug/ml streptomycin, 1mM sodium pyruvate and 1x GluteMax.

3. Results

3.0) Proteomic overlay analysis reveals ANXA6 and CD44 as candidate skeletal muscle derived exercise responsive sEV markers

The use of proteomic datasets was adopted as a hypothesis generating methodology with the aim of understanding the role of skeletal muscle in its contribution to the EV proteome during exercise. Adopting a conservative re-analysis of quantitative proteomic data to ensure high confidence in protein identification from EPS stimulated human myotube conditioned media (Laurens et al., 2020) and EVs isolated in human exercise arterial plasma (Whitham et al., 2018), resulted in the identification of 39 (Table S1) and 120 (Table S2) proteins significantly upregulated in their secretion, respectively (Figure 5A). These proteins shown to be upregulated from stimulated primary muscle cells and released into the circulation with exercise were cross referenced and filtered against non-quantitative proteomic datasets regarding skeletal muscle proteome (Deshmukh et al., 2015), C2C12 sEV proteome (Forterre et al., 2014) and the Vesiclepedia (Kalra et al., 2012) and Exocarta (Keerthikumar et al., 2016) databases. From this categorical breakdown, 5 proteins were identified to be abundant in mouse skeletal muscle tissue and C2C12 myotube sEVs that were also exercise responsive through *in vitro* muscle stimulation and *in vivo* in EVs from human plasma (Figure 5B, Table 5). Of these 5 proteins HEL-S-70 and CAP were disregarded due to their presence as protein isoforms; ATP1A1 was disregarded due to its identification as a potential putative exosome marker through its expression amongst multiple different cell lines in Kugeratski et al., (2021) dataset, and is therefore not muscle specific. Thus, CD44 and ANXA6 were hypothesized as candidate protein markers of skeletal muscle sEV secretion *in vivo* and were considered for further analysis.

Figure 5.

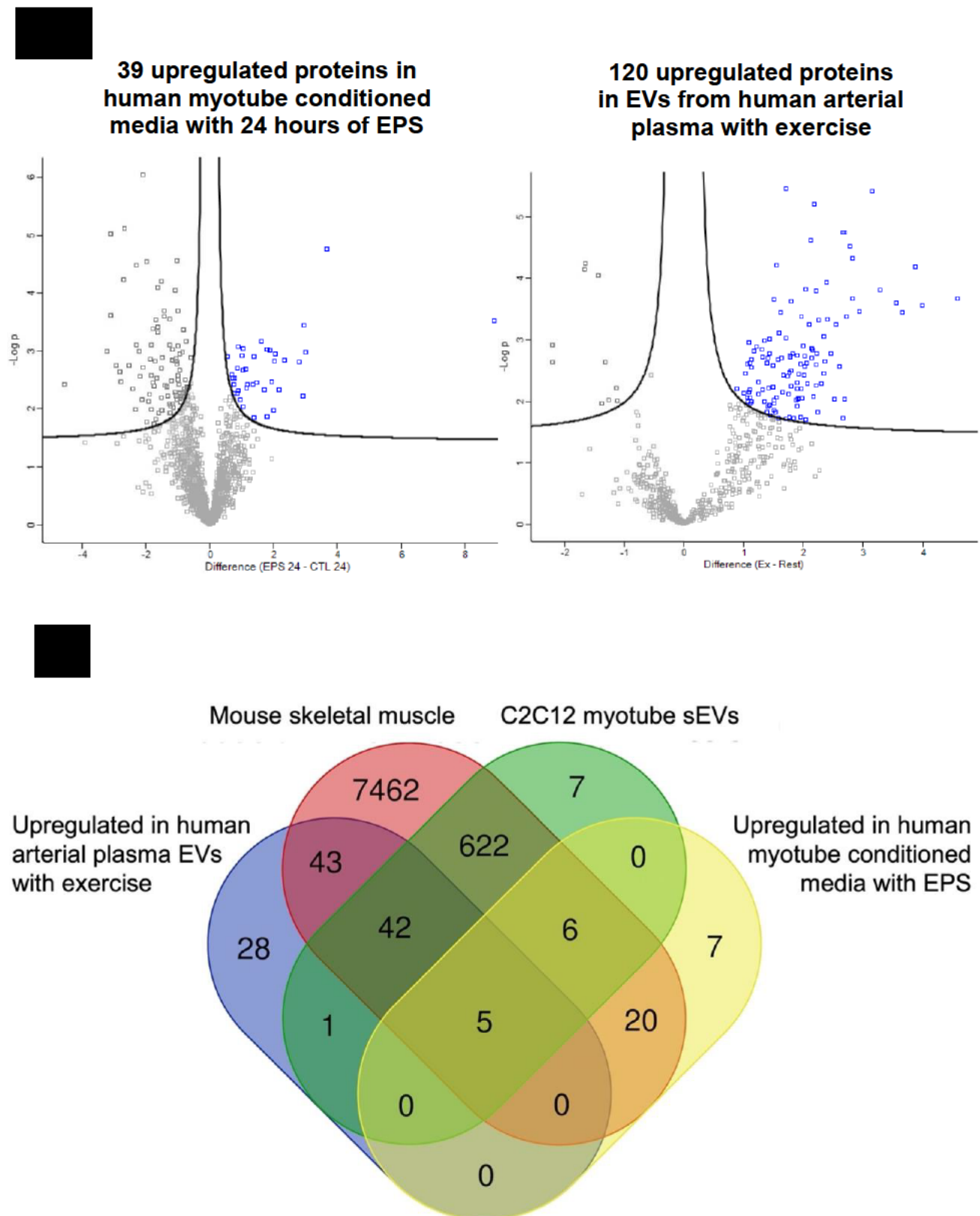


Table 5. Proteomic Overlay: ANXA6 and CD44 as candidate protein markers

Description: Proteins significantly upregulated with an exercise stimulus from human myotubes in conditioned media and EVs from human arterial plasma, that are also identified in a deep proteomic analysis of mouse skeletal muscle, C2C12 myotube sEVs, VesiclePedia and ExoCarta.

Protein Name	Gene Name
Annexin A6	ANXA6
CD44 antigen	CD44
Sodium/potassium-transporting ATPase subunit alpha-1; Sodium/potassium-transporting ATPase subunit alpha-3	ATP1A1:ATP1A3
Transitional endoplasmic reticulum ATPase	HEL-S-70;VCP;DKFZp434K0126
Adenylyl cyclase-associated protein	CAP

Figure 5. Proteomic Overlay: ANXA6 and CD44 as candidate markers of skeletal muscle sEV secretion during exercise (A) Re-analysis of proteomic data from Laurens et al., (2020) and Whitham et al., (2018) highlights 39 and 120 proteins significantly upregulated with an exercise stimulus *in vitro* and *in vivo*. Volcano plots were generated with X axis = significant difference between groups against, Y axis = $-\log(t \text{ test } p \text{ value})$. Significant values were identified using a two-samples paired t-test, FDR = 0.05, S0 = 0.1. P values were considered significant at $P < 0.05$. (B) Overlay highlights 5 proteins common amongst all datasets. Venn diagram was produced from matching gene names from overlaying proteomic data.

3.1) ANXA6 and CD44 are components of myotube derived sEVs

In line with results from the proteomic overlay data, different sEV isolation methods were adopted to determine whether ANXA6 and CD44 are components of sEVs (Figure 6). Moreover, the mouse murine muscle cell line C2C12 were adopted to match criteria established by datasets analysed by proteomics (Forterre et al., 2014). Firstly, UC highlighted that ANXA6 and CD44 correspond to sEVs sedimented at high-speed UC. Mindful of the potential for co-isolation of contaminant, non-EV proteins with UC, these findings were supported by the adoption of SEC isolation. Here, samples were separated into fractions corresponding to their size, eluting sEVs into fractions 1 to 3, and non-EV components into fractions 4 to 7, from which ANXA6 and

CD44 expression corresponded to the expected EV fractions. Finally, IMP was used to provide a highly specific, purer isolation method in conjunction with the other two approaches. For this, magnetic beads expressing CD9, CD63 and CD81 isolated sEVs positive for the three tetraspanins. In this regard, ANXA6 and CD44 were detectable in sEVs expressing the three tetraspanin markers. For all three isolation methods, the expression of commonly used sEV markers ALIX, TSG101 and/or CD9 were also investigated; of which all sEV markers provide clear conformation of the isolation techniques. Therefore, CD44 and ANXA6 are present in myotube derived sEVs regardless of isolation method.

Figure 6.

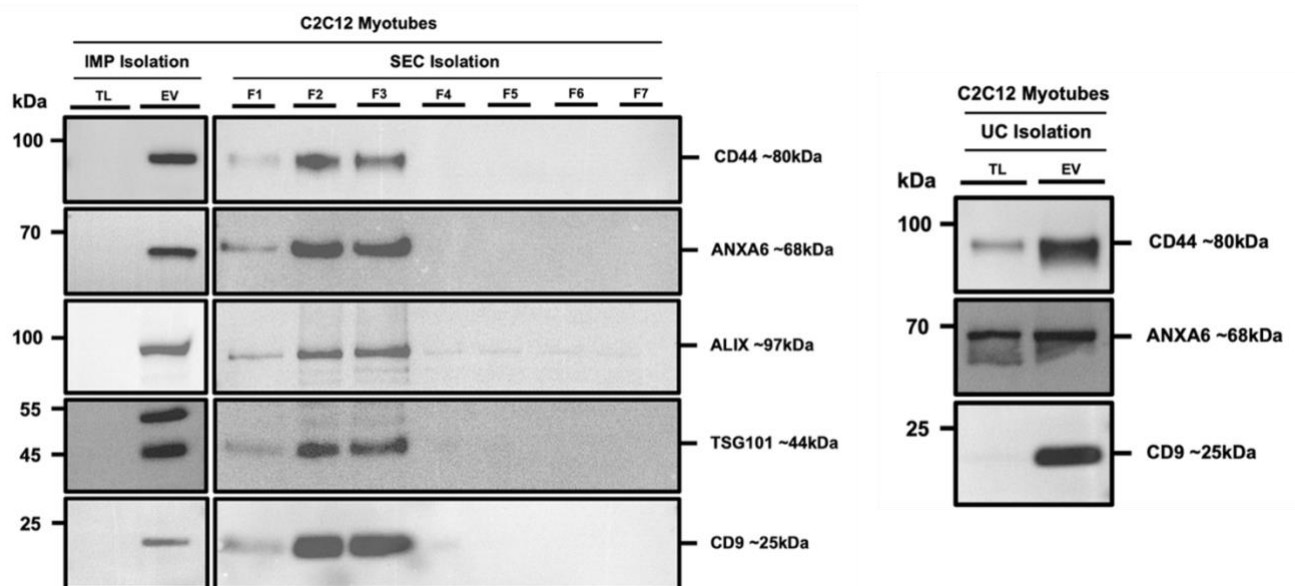
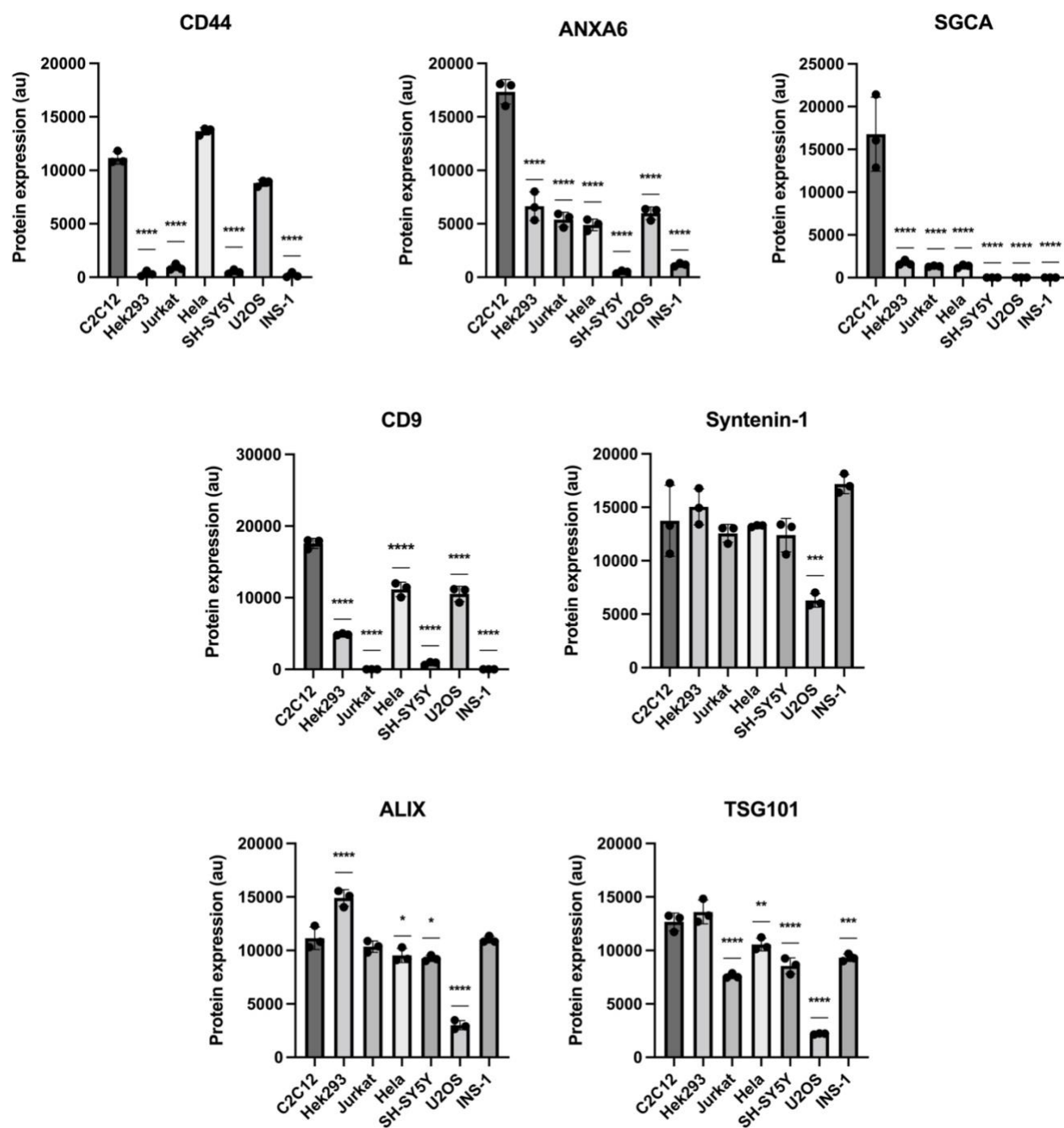


Figure 6. ANXA6 and CD44 are present in myotube derived sEVs. Immunomagnetic precipitation (IMP), size exclusion chromatography (SEC) and ultracentrifugation (UC) isolation of C2C12 myotube conditioned media highlights ANXA6 and CD44 as components of muscle derived sEVs. UC isolation indicates that ANXA6 and CD44 are abundantly expressed in sEVs. Similarly, SEC separation of sEV fractions 1 to 3 and non-EV fractions 4 to 7 indicates ANXA6 and CD44 as components of sEVs. sEV markers ALIX, TSG101 and/or CD9 were used as a conformation of isolation for the three techniques. Lastly, ANXA6 and CD44 are present in sEV lysates from IMP isolation CD9+, CD63+ and CD81+ vesicles compared to C2C12 myotube cell lysate. Data is presented as n = 1 (10ml conditioned media from 5 x 10cm dishes were pooled to produce 50ml total media, per n).

3.2) ANXA6 and CD44 are highly abundant but not unique to myotube sEVs

To understand the specificity of ANXA6 and CD44, and their potential roles as protein marker candidates in muscle derived sEVs, sEVs isolated by UC from C2C12 myotubes were compared to that of 6 different human immortalized cell lines (Figure 7). Analysis by immunoblotting revealed that ANXA6 and CD44 are abundantly expressed but not unique to C2C12 myotube sEVs. ANXA6 is enriched in C2C12 myotube sEVs compared to the other 6 cell lines ($P < 0.05$) but is not unique. CD44 is more specific to C2C12 myotube EVs compared to ANXA6, however it is also largely abundant in HELA and U2OS isolated sEVs. SGCA is a previously proposed muscle specific sEV marker (Guescini et al., 2015; Brahmer et al., 2019; Rigamonti et al., 2019) and as such was introduced as a comparator to our candidate markers ANXA6 and CD44. Interestingly, SGCA was largely unique to C2C12 myotube sEVs compared to the other cell lines ($P < 0.05$). In agreement with recent data from Kugeratski et al., (2021) Syntenin-1, ALIX and TSG101 are more universally expressed among multiple cell lines compared to commonly used sEV marker CD9. Together, SGCA appears to be uniquely expressed in C2C12 myotube sEVs compared to sEVs from other cell lines, whereas ANXA6 and CD44 appear to be abundantly expressed but not specific to myotube derived sEVs.

Figure 7.

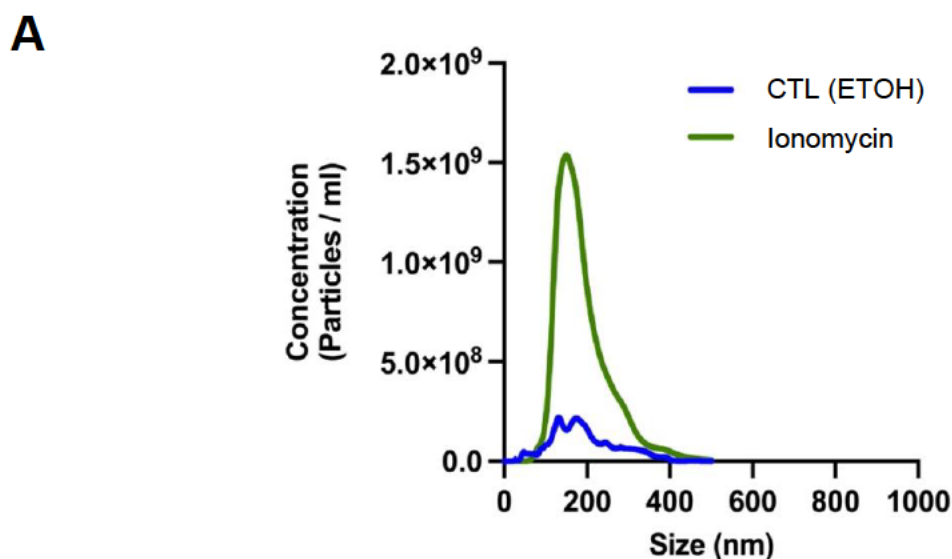


3.3) ANXA6 and CD44 are calcium responsive markers of sEV secretion from C2C12 myotubes stimulated *in vitro*

To comprehend the extent to which ANXA6, CD44 and SGCA are exercise responsive muscle sEV markers, C2C12 myotubes were mechanically and pharmacologically stimulated using EPS (Figure S1) and IM (Figure 8), respectively. In line with previous studies using the same protocol, EPS induced activation of cell signaling pathways in C2C12 myotubes associated with muscle contraction (Figure S1A) (Lambernd et al., 2012; Gogh et al., 2015). However, this model of EPS did not cause an increase in the expression of common sEV markers ALIX, TSG101, Syntenin-1 and CD9 indicative of sEV secretion (Figure S1B). As such, the lack of change in the expression of ANXA6 and CD44 by this method, was not unexpected (Figure S1B). As a result, it is inconclusive as to whether this model of EPS (2ms, 11.5V, 1hz) is sufficient for identifying the effects of contraction / exercise on muscle sEV secretion. Alternatively, IM causes an influx of calcium into the sarcolemma, mimicking increases in intracellular calcium concentrations with contraction and has previously been reported to alter gene and protein expression like that of exercise (Carter & Solomon, 2018). Furthermore, changes in intracellular calcium concentrations have been shown to mediate EV biogenesis and release (Savina et al., 2003; Mallick et al., 2015; Catalano & O'Driscoll, 2019; Taylor et al., 2020; Pecan et al., 2020) making calcium regulation during skeletal muscle contraction and EV release during exercise particularly interesting. NTA revealed a 4-fold increase in secreted particles with IM treatment compared to CTL (Figure 4A). Quantification of immunoblotting revealed that treatment of C2C12 myotubes with IM resulted in a significant increase in CD44 ($P < 0.05$, 180.69%), ANXA6 ($P < 0.05$, 158.29%) and TSG101 ($P < 0.05$, 93.61%) but not SGCA ($P = 0.6244$, 6.58%), compared to CTL in UC isolated sEVs (Figure 8B).

Therefore, this may suggest that an influx of intracellular calcium induced by a more robust stimulation with IM compared to EPS in C2C12 myotubes causes the secretion of sEVs expressing ANXA6 and CD44 as well as common sEV marker TSG101. Interestingly, although SGCA is largely unique to C2C12 myotube sEVs, it does not appear to be calcium responsive. Moreover, to determine that the effect of IM treatment on alterations in EV dynamics was not influenced by damage to myotube structure, images were taken daily from the start of myoblast differentiation into myotubes (Day 0), and throughout differentiation into fully formed myotubes (Day 6), as well as post IM treatment (Day 7) (Figure S2). From this, myotubes looked healthy and maintained classical tubular structures with no clear changes in morphology or excess cell death, post IM treatment. Therefore, it is unlikely that treatment disrupted myotube structure, implying that the effects seen are due to the treatment itself. Together, this suggests that the release of sEVs from C2C12 myotubes, is in part, calcium sensitive. From this, ANXA6 and CD44 might be better candidate markers compared to SGCA for the detection of muscle sEV secretion with an exercise stimulus *in vivo*.

Figure 8.



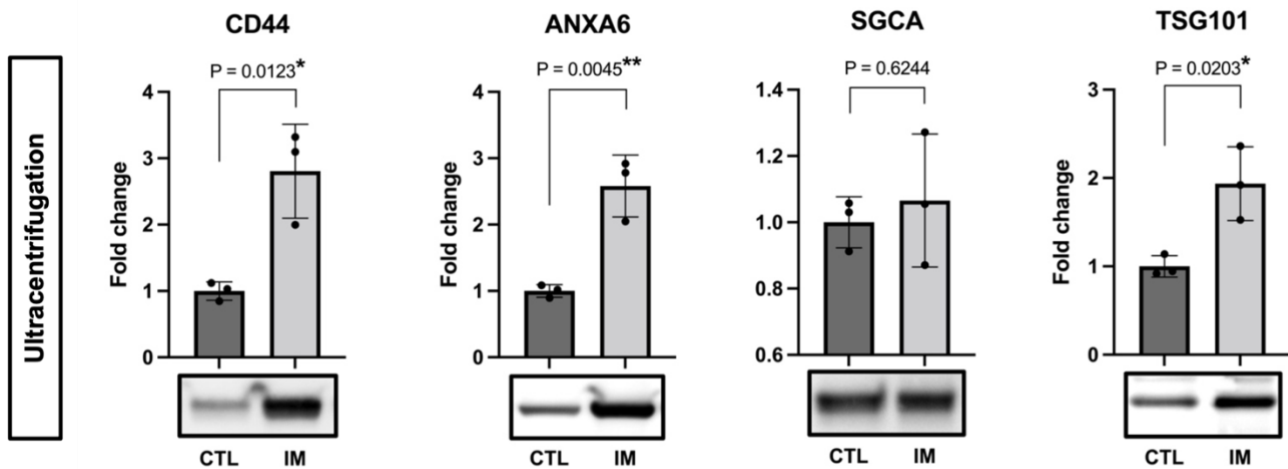
B

Figure 8. Ionomycin (IM) stimulation of myotubes induces secretion of sEVs which is reflected by increases in ANXA6+, CD44+ and TSG101+ sEVs *in vitro*.

(A) IM caused a 4-fold increase in secreted EVs. Particle concentrations were determined by nanoparticle tracking analysis (NTA) comparing IM and CTL conditions from $n = 3$. (B) IM treatment resulted in an increase in the abundance of sEV markers ANXA6, CD44 and TSG101. C2C12 myotubes were exposed to either IM treatment or control (CTL) vehicle (ethanol; ETOH) for 24 hours. Quantitative data produced from immunoblot images were subject to two-tailed unpaired t-test from $n = 3$ (10ml conditioned media from 5 x 10cm dishes were pooled to produce 50ml total, per n) per condition. Representative blots are shown below their respective quantifications. Data is presented as fold change relative to CTL for each protein marker. Individual data points and the mean \pm SD are shown; * = $P < 0.05$, ** = $P < 0.01$, *** = $P < 0.001$, **** = $P < 0.0001$.

3.4) Selective isolation of tetraspanin positive sEVs highlights CD44 as a potential candidate marker of sEV secretion with exercise *in vivo*

Since the expression of ANXA6 and CD44 in sEVs is calcium responsive *in vitro* through pharmacological stimulation of C2C12 myotubes; the next step to testing the hypothesis generated via unbiased proteomic data analysis was to confirm whether ANXA6+ and CD44+ sEVs increased in expression *in vivo* in human plasma after an exercise bout. A 200% Wmax HIIE cycling protocol was adopted in order to induce high levels of physiological stress to provoke a similar exercise sEV response as

previously reported (Vanderboom et al., 2021). As a conformation of protocol, pre- and post-exercise plasma was analyzed by ExoView; a single EV microarray capture technique by which CD9+, CD63+ and CD81+ sEVs are bound to on chip antibodies and fluoresced through the additions of secondary antibodies (CD9, CD63 and CD81) (Figure S3A). From this, individual counts for CD9+, CD63+ and CD81+ sEVs were totaled across all three capture spots for both pre and post exercise analysis (Figure 9A; Figure S3B). As expected, quantification and statistical analysis of pre- and post-exercise plasma showed a significant increase in the number of CD9+ ($P < 0.05$, 28.28%), CD63+ ($P < 0.05$, 68.64%) and CD81+ ($P < 0.05$, 13.16%) sEVs immediately post exercise. This indicates that the exercise protocol elicits an increase in circulating sEVs like that of previous studies (Fruhbeis et al., 2015; Whitham et al., 2018; Brahmer et al., 2019; Vanderboom et al., 2021; Kobayashi et al., 2021). Next, plasma was subject to either IMP or UC isolations pre- and post-exercise from the same protocol to investigate whether ANXA6+ and CD44+ sEVs are exercise responsive, *in vivo* (Figure 9B). Quantification of immunoblotting from sEVs isolated by UC in exercise plasma highlights an increase in circulating CD44 (33.82%) pre-post exercise protocol, however, it did not reach statistical significance ($P = 0.1002$). No significant changes were observed pre-post exercise for ANXA6 or SGCA ($P = 0.7138$ and $P = 0.8874$, respectively). IMP isolation highlighted a significant increase pre-post exercise in circulating CD44+ ($P < 0.05$, 879.84%) vesicles with no significant changes in ANXA6 or SGCA ($P = 0.9933$ and $P = 0.6960$, respectively). In conclusion, CD44+ sEVs isolated by IMP are exercise responsive under high intensity conditions *in vivo* in human plasma.

Figure 9.

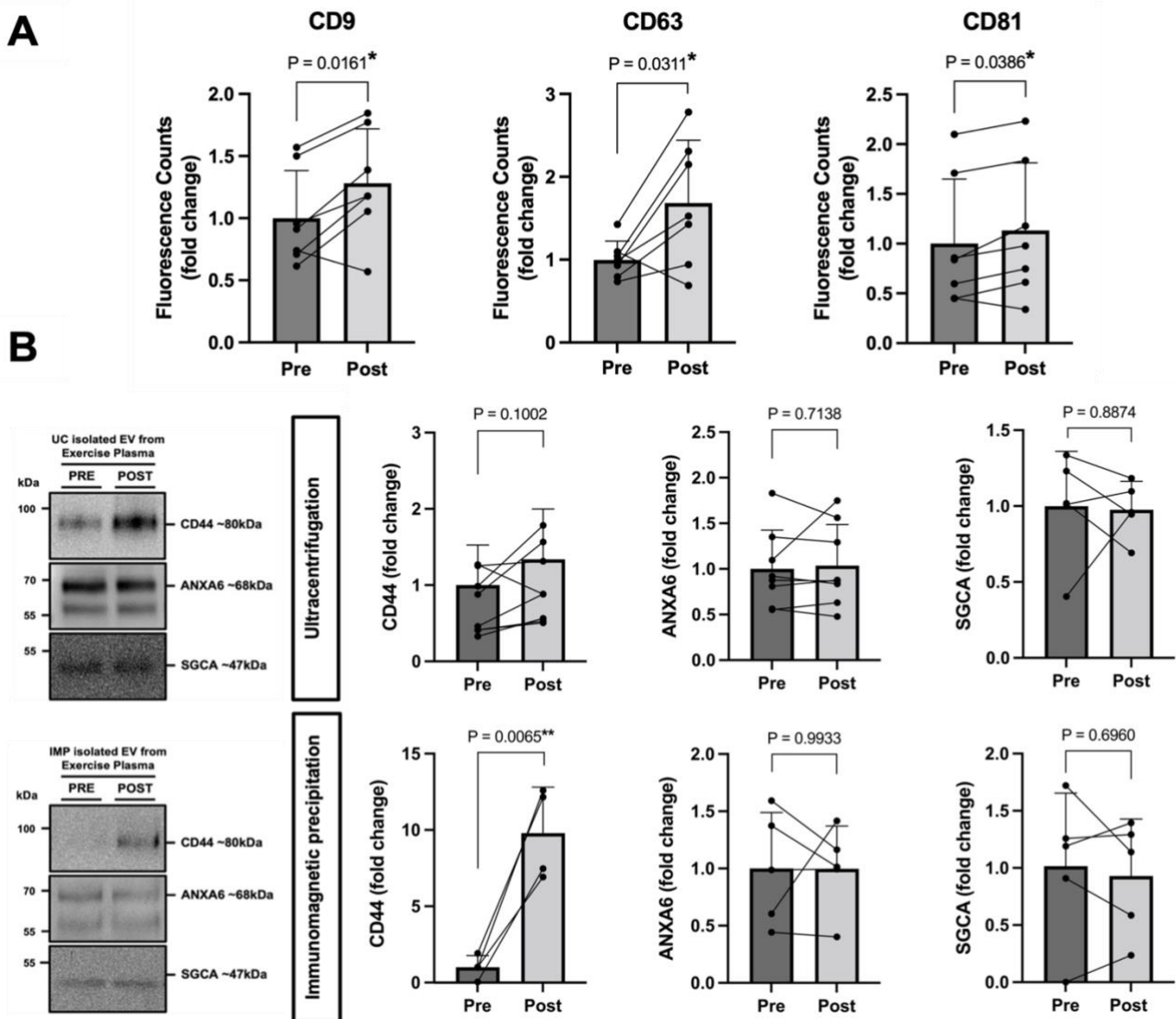


Figure 9. High intensity interval exercise (HIE) causes an increase in circulating sEV markers CD9, CD63, CD81 as well as IMP isolated CD44+sEVs. (A) ExoView analysis reveals an increase pre-post exercise in CD9+, CD63+ and CD81+ vesicles typical of the exercise sEV response. Pre- and post-exercise plasma samples were exposed to on chip ExoView analysis by single EV microarray capture and fluorescence for CD9+, CD63+ and CD81+ vesicles. Data was produced from fluorescent counts on an individual EV basis from immunoaffinity capture calculating total CD9, CD63 and CD81 expression across all 3 capture spots. Data is presented as fold change between pre- and post-exercise relative to the mean of 'pre' of each group (CD9, CD63 and CD81, respectively). (B) IMP and UC isolation of pre- and post-exercise plasma reveal that CD44 is an exercise responsive marker under purer isolation conditions. Plasma from both conditions was exposed to either ultracentrifugation (UC) isolation or immunomagnetic precipitation (IMP) isolation for CD9+, CD63+ and CD81+ vesicles. Representative images for immunoblotting are shown for both UC and IMP pre- and post-exercise for each target protein. Quantitative data was subject to a two-tailed paired t-test comparing pre-post exercise. Data is presented as fold change relative to the mean of the 'pre' for each marker. Individual data points including mean \pm SD are shown; * = $P < 0.05$, ** = $P < 0.01$, *** = $P < 0.001$, **** = $P < 0.0001$.

4. Discussion

Defined protein markers that allow for the separation of EVs by tissue of origin (muscle vs adipose) or method of biogenesis (exosome vs microvesicle) are currently lacking in the field. Specifically, those that allow for the detection of skeletal muscle derived EVs. Discovery of proteins markers allowing for the clear segregation of EVs between various tissues and cells, permitting improved clarifications of their origins and uptake in various biological contexts (i.e., exercise, sedentary), would massively improve understanding as to their biological relevance. To date, it is inconclusive as to what extent skeletal muscle EVs contribute to the circulation. Studies have previously incited that changes in skeletal muscle EVs can be characterized by contrasts in the expression of SGCA (Guescini et al., 2015; Brahmer et al., 2019; Rigamonti et al., 2019). Although this may be somewhat true, the fact that myotube derived EVs contain hundreds of proteins (Forterre et al., 2015) makes it difficult to determine whether SGCA can account for all. Similarly, the fact that exercise causes considerable mechanical and metabolic perturbation, which has already been shown to alter the circulating EV secretome drastically (Whitham et al., 2018; Vanderboom et al., 2020), it is conceivable that the composition of skeletal muscle derived EVs might be modified in a similar manner. As such, previous assumptions of skeletal muscle EV protein markers which do not take into consideration global analysis and the perturbations of exercise, may be limited in discovery of other potential muscle sEV subpopulations.

4.0) Proteomic overlay highlights ANXA6 and CD44 as novel candidate markers of skeletal muscle EV secretion with exercise

To address these issues, the present study utilized publicly available proteomic data to evaluate novel candidate protein markers of EVs secreted by skeletal muscle.

Through re-analyzing and overlaying current datasets involving skeletal muscle tissue proteome, muscle derived EVs, and the influence of an exercise stimulus *in vitro* and *in vivo*, it was hypothesized that ANXA6 and CD44 were exercise responsive candidate markers of skeletal muscle sEV secretion (Figure 5A; Figure 5B).

4.1) Advantages of combining proteomics and targeted methods for skeletal muscle EV protein marker discovery

Previous work has elucidated the potential of SGCA, a highly abundant skeletal muscle protein, as a method of detecting skeletal muscle derived EVs (Guescini et al., 2015; Brahmer et al., 2019; Rigamonti et al., 2019). Notably, all these studies assume skeletal muscle EV secretion based on the presence of SGCA by immunoblotting alone (Guescini et al., 2015; Brahmer et al., 2019; Rigamonti et al., 2019) and a fundamental limitation of immunoblotting is its targeted nature, seeing as researchers can only identify what they are looking for (Mann, 2008). Fully quantitative proteomics on the other hand is adept at detecting a large proportion of proteins underlying pathological and physiological mechanisms, making it a much better method of biomarker and protein marker detection in biological fluids (Good et al., 2007). However, this must be tackled with caution, as the methodological approach of sample preparation before mass spectrometry can limit protein detection and affect analysis (Garbis, Lubec & Fountoulakis, 2005). As such, the presence or absence of a protein, might not be truly reflective of its secretion or uptake from a tissue. However, as proteomics rapidly uncovers the vast network of the human protein atlas and how this network is affected throughout the body, in response to exercise, cross referencing multiple proteomic datasets, as highlighted in the present study, becomes a more effective tool for understanding specific protein interactions within different biological

contexts. Together, this provides greater confidence for targeted analyses when generating hypotheses. Which produced the rationale for the present study and should be considered by others, should the aim be protein marker identification. In this regard, the present studies proteomic overlay informed the targeted methodological approaches taken in evaluating ANXA6 and CD44 as markers of skeletal muscle sEV secretion with exercise.

Since the proteomic data used in the present analysis concerning both muscle and plasma EV bound proteins from Forterre et al., (2015) and Whitham et al., (2018), respectively, were both generated via different UC isolation protocols, it was conceivable that ANXA6 and CD44 were detected as artifacts or contaminants of isolation. Moreover, as previously discussed, different isolation methods enable differing results in terms of sEV purity and yield (Brennan et al., 2020). As such, confirmation of the incorporation of ANXA6 and CD44 into sEVs was highlighted amongst sEVs isolated by UC, SEC, and IMP (Figure 6). In addition, the presence of markers ALIX, TSG101, Syntenin-1 and CD9 were adopted to confirm the ability of the three methodologies to isolate myotube sEVs.

4.2) SGCA is a highly unique myotube EV marker

Markedly, SGCA was highly unique to C2C12 myotube derived sEVs when compared to EVs isolated from several human derived cell lines, whereas ANXA6 and CD44 were not (Figure 7). Through an online search of the human protein atlas (Uhlen et al., 2015), it is evident that ANXA6 and CD44 are ubiquitously expressed in a multitude of cells and tissues around the body. ANXA6 and CD44 are involved in membrane organization / trafficking and cell-cell interchange by means of regulation of the

extracellular matrix (ECM), respectively. Additionally, CD44 is a transmembrane glycoprotein (Goodison, Urquidi & Tarin, 1999), whereas ANXA6 participates in membrane regulation through calcium-dependent binding mechanisms (Gerke, Creutz & Moss, 2005). In combination with an understanding of their functionality, their incorporation into EVs is not surprising. Similarly, CD44 has been shown to participate in tumor progression, metastasis, and proliferation (Senbanjo & Chellai, 2017), and has been shown to be involved in the progression of osteosarcoma in bone (Gao et al., 2015; Mayr et al., 2017; Senbanjo & Chellaiah, 2017; Liu et al., 2018) and cervical cancers (Zhang et al., 2019; Abdel-Hamid et al., 2021) and by its very nature its detection in U2OS and HELA derived sEVs is not unexpected. Importantly, CD44 and ANXA6 have been characterized to be involved in myogenesis (Mylona et al., 2006; Meligy et al., 2012; Scimeca et al., 2015; Leng et al., 2019) and muscular plasma membrane repair (Demombreun et al., 2016; Demombreun et al., 2019; Croissant et al., 2020), respectively. Despite their contribution to other cell derived sEVs, myotubes still incorporate ANXA6 and CD44 as part of sEVs (Figure 7) meaning an increase in their abundance in circulating sEVs may be reflective of skeletal muscle secretion during exercise.

4.3) Syntenin-1 is a better candidate putative marker of exosomes compared to canonical tetraspanin marker CD9

In addition to the detection of ANXA6, CD44 and SGCA, the expression of EV markers ALIX, TSG101, Syntenin-1 and CD9 was also examined across the several different cell lines. From this, it was evident that ALIX, TSG101 and Syntenin-1 were all more ubiquitously expressed across the different cell lines in comparison to classically proposed exosomal marker CD9 (Figure 7). Due to their role in ILV formation, the

tetraspanin markers CD9, CD63 and CD81 have long been used as biomarkers for exosome detection and classification (Kowal et al., 2016; Jeppesen et al., 2019). In a recent paper, Kugeratski et al., (2021) adopted super-SILAC-based MS analysis of exosomes isolated from 14 human cell lines to identify putative exosome/sEV markers. Like that of the present study's findings, the authors noticed that CD9, CD63 and CD81 were heterogeneously expressed across exosomes from the 14 different cell lines, and as such were not classified as putative exosome markers. From this analysis, it was identified that Syntenin-1 was the most abundantly expressed exosomal marker throughout all cell lines (Kugeratski et al., 2021). The data presented in the present study supports the notion that Syntenin-1 is a universal exosome/sEV marker (Figure 7) and should be used, in combination with other markers (i.e., ALIX, TSG101), for proper clarification of exosome isolation.

4.4) Myotube secretion of sEVs is calcium sensitive *in vitro*

Regardless to what extent EVs are secreted locally or within the circulation by muscle, the mechanisms by which skeletal muscle regulates EV biogenesis and release, are unknown. Although multiple groups report the effectiveness of *in vitro* muscle contraction by EPS on the secretion of myokines, such as IL-6 (Lambernd et al., 2012; Gogh et al., 2015; Barlow, Carter & Solomon, 2018; Lautaoja et al., 2021), comparatively, this is the first attempt at measuring EV dynamics from C2C12 myotubes stimulated by EPS. Despite observing alterations in the phosphorylation of AMPK, ERK1/2 and p38 (Figure S1A), proteins known to be phosphorylated with contraction, this did not translate into changes in the expression of sEV markers ALIX, TSG101, Syntenin-1 and CD9 (Figure S1B). Estrada et al., (2021) observed a similar response when applying electrical stimulation *ex vivo* to mouse extensor digitorum

longus muscle, from which the abundance of sEVs secreted into the conditioned media was not altered by contraction. Similarly, the authors reported that pharmacological inhibition of contraction in primary mouse skeletal muscle through administration of blebbistatin, an ATPase inhibitor, did not alter the total number of sEVs secreted (Estrada et al., 2021). Initially, this warrants questions as to the reliability of this methodology to replicate contraction / exercise stimulated EV secretion. It would have been beneficial in the present study to investigate EPS on human primary muscle to confirm findings by Estrada et al., (2021) and to match the proteomic data adopted from the Laurens et al., (2012) paper as a method of validation. As such, this is a limitation of the present study. However, this does provide evidence that skeletal muscle secretion of EVs may be due to different stimuli and not just that of mechanical contraction alone.

Changes in intracellular calcium have previously been shown to contribute to the regulation of EV biogenesis and release (Savina et al., 2003; Mallick et al., 2015; Catalano & O'Driscoll, 2019; Taylor et al., 2020; Pecan et al., 2020). The concept that EV formation and secretion from skeletal muscle during exercise might be in part, due to the influx of calcium into the sarcolemma to induce actin-myosin crossbridge formation during the process of contraction, is one of interest. Notably, Fujita, Nedachi and Kanaki, (2007) identified that 6 hours of EPS at 40V, 1hz, 24ms caused significant changes in calcium influx and calpain activity. Similarly, Olsson et al., (2015), highlighted that myotubes displayed a distinct lack of fundamental calcium handling due to discrepancies in the quantity and organization of calcium handling proteins (RyR, DHPR, SERCA1 and SERCA2) in the sarcomere compared to that of intact human muscle fibers. As such, the reduced capacity to generate sufficient calcium

influx limits the ability of myotubes to contract to the same forces as human myofibers *in vitro* (Olsson et al., 2015). It may be speculated that a lower voltage (11.5V) and frequency (1ms), coupled with the use of C2C12 myotubes in the current analysis hindered sEVs secretion as a consequence of limited changes in intracellular calcium. To understand the potential for calcium as a regulator of EV biogenesis and secretion from muscle cells *in vitro*, the calcium ionophore, IM was adopted to stimulate significant changes in intracellular calcium concentrations of C2C12 myotubes *in vitro*. The present study identified a ~4-fold increase in the release of UC isolated sEVs as detected by NTA after 24 hour incubation with IM compared to control vehicle (Figure 8A). In addition to this, increases were also observed in the expression of ANXA6+ (~2.6-fold) and CD44+ (~2.8-fold) sEVs (Figure 8B). In this regards, sEV secretion from myotubes seems to be in part, calcium sensitive and therefore may present a method linking contraction induced calcium influx into the sarcolemma with skeletal muscle sEV biogenesis and release *in vivo* during exercise. However, the present study is limited by a lack of sample size (n = 3) and as such conclusions must be made with caution of reporting a type 2 error. Similarly, the present study would have profited from a confirmation that ionomycin treatment activated intracellular calcium signalling such as measurements of the phosphorylation of CAMK-related intracellular signalling proteins. Although, previous studies have highlighted the robustness of this methodology and is evident in a review by Carter & Solomon (2018). Nevertheless, this does permit further research to focus on the role of calcium in sEV biogenesis and release from skeletal muscle under contractile and/or exercise conditions.

4.5) HIIE causes an increase in circulating tetraspanin positive sEVs

In line with our hypothesis generated by proteomics, the next step was to measure the ability of ANXA6 and CD44 to represent exercise responsive sEV markers *in vivo*. Validation of replication of the acute exercise sEV response previously observed in other studies (Fruhbeis et al., 2015; Whitham et al., 2018; Brahmer et al., 2019; Vanderboom et al., 2021; Kobayashi et al., 2021) was achieved through the use of ExoView analysis, a single EV microarray capture technique that allows for the quantification of the expression of CD9+, CD63+ and CD81+ vesicles through fluorescence on a singular EV bases (Figure S3A). A useful benefit of this technique is the lack of prior purification steps needed before application due to the binding of specific antibodies. This provides a high purity methodology of detecting sEVs based on the three tetraspanin markers, providing details for both particle counts and intensity of expression. From this, HIIE caused a significant increase in circulating tetraspanin positive sEVs, providing validation of the exercise protocol (Figure 9A; Figure S3B).

4.6) The purity of isolation method effects the clarity of observed changes in sEV marker dynamics with HIIE *in vivo*

Significant increases were only observed in CD44+sEVs isolated by IMP compared to UC (Figure 9B). This may be explained by that fact that UC is a cruder method of isolation that offers higher yield with lower purity. Due to the similar size, density and sedimentation properties of other vesicles (i.e., lipoproteins), protein contaminants (i.e., albumin) and aggregates (György et al., 2011), especially in the context of blood plasma, immunoblotting alone may not be sensitive enough to detect changes amongst EVs, contaminants, and aggregates through this method of isolation. Seeing

as the hypothesis was generated through proteomics, a much more sensitive technique that is able to distinguish with greater clarity the differences in protein abundance between the conditions, the use of immunoblotting in the present study, a less sensitive technique, may explain the lack of modification detected in ANXA6+sEVs and CD44+sEVs with UC isolation post exercise (Figure 9B).

Comparatively, IMP provides a targeted method of isolation that eliminates a larger proportion of co-isolated unwanted contaminants through higher selectivity which improves the transparency in the observed effects (Carnino, Lee and Jin, 2019). As such, the expression of CD44 that co-isolated with CD9+, CD63+ and CD81+ sEVs in human plasma after exercise increased ~8.8-fold (Figure 9B). Interestingly, SGCA was detectable through both UC and IMP in exercise plasma (Figure 9B) which agrees with previous work by Guescini et al., (2015) and Rigamonti et al., (2019), suggesting that SGCA+sEVs do contribute, even if minimally, to the circulation. However, like that of findings by Brahmer et al., (2019), exercise did not alter the expression of circulating SGCA+sEVs *in vivo* (Figure 9B).

4.7) SGCA may represent a non-exercise responsive marker of skeletal muscle sEV secretion

SGCA was non-detectable by re-analysis of proteomic data regarding the 39 proteins significantly upregulated in the conditioned media after 24 hour EPS stimulation of human primary myotubes (Figure 5A; Table S1), nor was it discovered in the 120 proteins upregulated in EVs isolated from human plasma after exercise (Figure 5A; Table S2). In agreement with these findings SGCA was not exercise responsive by targeted methods, *in vitro* (Figure 8) or *in vivo* (Figure 9). Despite appearing to be

largely unique to myotube derived sEVs (Figure 7), the expression of SGCA remained constant when *in vitro* stimulation by IM appeared to significantly upregulate the secretion of sEVs detected by NTA (Figure 8A) which corresponded with increases in ANXA6, CD44 and canonical marker TSG101 (Figure 8B). From this, it may be suggested that, although SGCA is a good marker of muscle sEV secretion in the basal state, it is not representative of the potential for skeletal muscle to secrete sEVs with exercise. This is also evident in previous reports where groups have failed to identify differences in the expression of SGCA+sEVs with acute exercise *in vivo* by similar methods (Brahmer et al., 2019). Although, this hypothesis is limited to the concept that if SGCA is ubiquitously expressed across all skeletal muscle derived sEVs then the process of normalizing to total protein may be disregarding any changes observed by immunoblotting. However, drastic alterations in the expression of CD44+sEVs *in vitro* (Figure 8B) and *in vivo* (Figure 9B) with an exercise stimulus warrants further investigation into its possibility as an exercise responsive muscle derived sEV marker.

4.8) The potential role of ANXA6 and CD44 in sEVs secreted from myotubes

It is conceivable that the detection of ANXA6 and CD44 *in vivo* human plasma is still representative of skeletal muscle derived sEVs, seeing as they are highly enriched in myotube sEVs (Figure 7) and expressed in the proteomic overlay (Figure 5B; Table 5). However, this is difficult to conclude in the present study due to their lack of specificity to myotube sEVs in the basal state compared to other cell lines (Figure 7). Yet, regardless of whether they are liberated into the circulation, the cross referencing of proteomics from C2C12 myotube sEVs and human myotubes stimulated by 24 hours of EPS (Figure 1B), reinforced by *in vitro* stimulation of C2C12 myotubes via the calcium ionophore IM, highlighted the release of ANXA6+ and CD44+ sEVs from

skeletal muscle into the extracellular space (Figure 8B). Interestingly, CD44 is prevalent in early stage myogenin differentiation as well as myoblast proliferation and differentiation through motility of myoblasts to fuse and become multinucleated myotubes by directing cytoskeletal dynamics in the ECM (Mylona et al., 2006; Meligy et al., 2012; Scimeca et al., 2015; Leng et al., 2018). Similarly, it has been suggested that ANXA6 is involved in skeletal muscular repair through plasma membrane resealing after laser-induced membrane ablation, thought to replicate injury following forced contraction (Demombreun et al., 2016; Demombreun et al., 2019; Croissant et al., 2020) and is inhibited in muscular dystrophy models (Demonbreun et al., 2016). From this, it may be speculated that skeletal muscle releases ANXA6+ and CD44+ sEVs as a method that might link the onset of contraction with EVs release to regulated ECM dynamics, myogenic activation, and skeletal muscle repair, as previously hypothesized by Bittel & Jaiswal (2019). However, this requires further research and remains as speculation. Seeing as recombinant ANXA6 treatment has been shown to improve membrane repair against muscle injury (Demombreun et al., 2016) it may be interesting to compare these results against treatment with muscle sEVs overexpressing ANXA6 to see if improvements in membrane repair can be recapitulated. A similar approach could be adopted for CD44. This hypothesis agrees with recent findings by Mytidou et al., (2020) that skeletal muscle secretes EVs as a method of local skeletal muscle crosstalk. As such, they may work as a manner of regulating muscle repair. However, seeing as this has not yet been studied in an exercise context, the exact functionalities of local skeletal muscle communication are not yet clear.

4.9) Local and/or distal crosstalk of skeletal muscle derived EVs: A need for further research

Due the lack of methodology allowing for the absolute separation of skeletal muscle EVs compared to other cells and tissues in the body, it is still unclear as to what extent they contribute to the circulation. The current working hypothesis is that a large portion of skeletal muscle secretion is restricted to local communication (Mytidou et al., 2021; Estrada et al., 2021). sEVs isolated from the hindlimbs of mice express muscle enriched myomiRs, miR-1, -133a, -133b and -206, of which the concentrations of EVs incorporating the four myomiRs in plasma, were considerably lower than that of endogenously derived EVs from muscle (Mytidou et al., 2021), insinuating limited transfer of such sEVs to the circulation. Furthermore, downregulation of miR-133b in the tibialis anterior affected miR-133b expression in proximal (gastrocnemius), but not distal muscles (triceps), suggesting that transfer of EVs containing miR-133b occurs locally. However, much like the detection of a singular protein (i.e., SGCA), it is difficult to determine whether a singular miRNA is indicative of all skeletal muscle EV populations. In recent work by Estrada et al., (2021), through the breeding of a mice colony expressing specific incorporation of mG (membrane target enhanced GFP) into skeletal muscle (due to the presence of Cre recombinase) and mT (membrane target dimer Tomato) in all other tissues, the authors detected 0.26% of circulating sEVs containing mG only, suggestive of skeletal muscles contribution to the circulation. Whereas 99.4% of EVs derived from skeletal muscle *ex vivo*, incorporated mG (Estrada et al., 2021). Seemingly, this provides evidence that in the basal state, skeletal muscle secretes EVs with the primary function of local communication (Mytidou et al., 2021; Estrada et al., 2021). However, seeing as pharmacological and mechanical stimulation of muscle *in vitro* has the capability to alter protein composition

of sEVs (Figure 8B) and secreted proteins (Figure 5A, Table S1) it is conceivable that this may not be the case with an exercise stimulus. Whitham et al., (2018) reported 35 EV bound proteins, of which 15 did not contain a signaling peptide, with significant rates of release from the exercising limb, as identified by changes in protein expression in arteriovenous balance analyzed pre and post exercise. As such, measurements of EVs in the basal state, as is the case with many current studies (Forterre et al., 2014; Estrada et al., 2021; Mytidou et al., 2021) may not be reflective of the potential for skeletal muscle to secrete EVs into the circulation for distal communication during exercise. With an understanding that the Estrada et al., (2021) model of mG tagging of skeletal muscle sEVs allows for specific detection in the circulation, it would be beneficial to apply this to an exercise setting to understand how this alters skeletal muscles contribution to the circulation and to help comprehend where these EVs may be targeted to. Similarly, the current hypothesis that sEVs secreted from muscle are primarily targeted locally is limited to mouse models without an understanding of how these finding may translate in humans. An advantage of the present study is the identification of *in vitro* exercise responsive markers that translate across species. Therefore, ANXA6 and CD44 may be implemented as markers that allow for the measurements of sEV release from primary human myotubes and mouse C2C12 myotubes, with an exercise stimulus.

Chronic exercise has been shown to modulate circulating EV bound miRNA content through the upregulation of miR-133a, -133b and -206 after a 5-week high intensity exercise program, in mice (Castano et al., 2020), of which similar increases have been reported to correlate with aerobic fitness in humans (Guescini et al., 2015). Seeing as only 6 proteins were significantly upregulated in the circulation with an acute bout of

resistance exercise (Vanderboom et al., 2021), in conjunction with the lack of evidence as to whether there is an increased release of sEVs from skeletal muscle with aerobic exercise, it is plausible that repeated exercise causes gradual changes in skeletal muscle derived sEV content independent of absolute changes in the concentration of sEVs secreted from the tissue with an acute bout of exercise. In this regards, acute modifications in the packaging of proteins (Whitham et al., 2018; Vanderboom et al., 2021), metabolites (Whitham et al., 2018) and miRNAs (Guescini et al., 2015; Castano et al., 2020) in EVs from skeletal muscle, may result in more permanent alterations in the EV proteome with chronic exercise, resulting in adaptations in other tissues around the body; which has already been shown through the 4-week injection of exercise derived EVs isolated from the skeletal muscle interstitial fluid of donor mice into sedentary mice which exerted significant improvements in glucose tolerance in comparison to EVs isolated from liver under the same conditions (Castano et al., 2020). As such, chronic modifications in protein and miRNA sorting in exercise derived EVs brought about by repetitive exercise is an area that needs investigating for its potential implementation in the context of adaptation and disease suppression.

4.10) Conclusion

There is growing evidence to suggest that skeletal muscle secreted sEVs have the capability of interacting locally (Estrada et al., 2021; Mytidou et al., 2021) and distally via the circulation (Whitham et al., 2018; Castano et al., 2020) through the transfer of proteins and miRNAs that can potentially mediate skeletal muscle repair and myogenesis (Forterre et al., 2015; Bittel & Jaiswal, 2019) and improvements in hepatic glucose and insulin tolerance (Castano et al., 2020). However, these findings remain as speculation due to the lack of methodology allowing for clear separation of myotube

derived sEVs from any other cell or tissue in the body. It is inconclusive as to whether ANXA6 and CD44 are representative of skeletal muscle derived sEV secretion with exercise *in vivo* due to their lack of specificity to myotube sEVs. Nevertheless, they may be good markers of secretion *in vitro*, and therefore warrant further investigations into their role in skeletal muscle sEV secretion with exercise or contraction. More so, calcium may act as a stimulant for sEV biogenesis and release from skeletal muscle, coupling contraction and secretion of sEVs locally, and potentially distally, during exercise. Finally, the present study highlights the advantages of adopting global analysis by proteomics to generate hypotheses that inform targeted methods for the discovery and validation of protein candidate markers of tissue specific sEV secretion. Furthermore, research should aim to continue collecting and advancing proteomic data concerning the complexity of skeletal muscle sEVs as well as sEVs derived from all other tissues around the body under both basal and exercise conditions. Over time, the culmination of proteomic data regarding the EV protein network during exercise will allow for a much more in-depth comprehension of tissue specific EV protein sorting and protein marker discovery with exercise. Together, this will permit a greater understanding of skeletal muscle EV contribution and distribution to local and/or distal tissues during exercise induced crosstalk.

5. References

- Abdel-Hamid, N. M. *et al.* (2021) 'Identification of Chemo and Radio-Resistant Sub-Population of Stem Cells in Human Cervical Cancer HeLa Cells', *Cancer Investigation*, 39(8), pp. 661–674. doi: 10.1080/07357907.2021.1931875.
- Akers, J. C. *et al.* (2013) 'Biogenesis of extracellular vesicles (EV): exosomes, microvesicles, retrovirus-like vesicles, and apoptotic bodies', *Journal of neuro-oncology*, 113(1), pp. 1–11. doi: 10.1007/S11060-013-1084-8.
- Aswad, H. *et al.* (2014) 'Exosomes participate in the alteration of muscle homeostasis during lipid-induced insulin resistance in mice', *Diabetologia*, 57(10), pp. 2155–2164. doi: 10.1007/S00125-014-3337-2/FIGURES/8.
- Aswad, H., Jalabert, A. and Rome, S. (2016) 'Depleting extracellular vesicles from fetal bovine serum alters proliferation and differentiation of skeletal muscle cells in vitro', *BMC biotechnology*, 16(1). doi: 10.1186/S12896-016-0262-0.
- Bæk, R. *et al.* (2016) 'The impact of various preanalytical treatments on the phenotype of small extracellular vesicles in blood analyzed by protein microarray', *Journal of Immunological Methods*, 438, pp. 11–20. doi: 10.1016/J.JIM.2016.08.007.
- Balci, B. and Dinçer, P. (2009) 'Efficient transfection of mouse-derived C2C12 myoblasts using a matrigel basement membrane matrix', *Biotechnology journal*, 4(7), pp. 1042–1045. doi: 10.1002/BIOT.200800269.
- Bei, Y. *et al.* (2017) 'Exercise-induced circulating extracellular vesicles protect against cardiac ischemia-reperfusion injury', *Basic research in cardiology*, 112(4). doi: 10.1007/S00395-017-0628-Z.
- Bendtsen, J. D. *et al.* (2004) 'Feature-based prediction of non-classical and leaderless protein secretion', *Protein engineering, design & selection : PEDS*, 17(4), pp. 349–356. doi: 10.1093/PROTEIN/GZH037.

- Bertoldi, K. *et al.* (2018) 'Circulating extracellular vesicles in the aging process: impact of aerobic exercise', *Molecular and Cellular Biochemistry*, 440(1–2), pp. 115–125. doi: 10.1007/S11010-017-3160-4/FIGURES/8.
- Bittel, D. C. and Jaiswal, J. K. (2019) 'Contribution of extracellular vesicles in rebuilding injured muscles', *Frontiers in Physiology*, 10(JUN). doi: 10.3389/fphys.2019.00828.
- Bodega, G. *et al.* (2019) 'Microvesicles: ROS scavengers and ROS producers', <https://doi.org/10.1080/20013078.2019.1626654>, 8(1). doi: 10.1080/20013078.2019.1626654.
- Booth, F. W., Roberts, C. K. and Laye, M. J. (2012) 'Lack of exercise is a major cause of chronic diseases', *Comprehensive Physiology*, 2(2), pp. 1143–1211. doi: 10.1002/CPHY.C110025.
- Brahmer, A. *et al.* (2019) 'Platelets, endothelial cells and leukocytes contribute to the exercise-triggered release of extracellular vesicles into the circulation', *Journal of Extracellular Vesicles*, 8(1). doi: 10.1080/20013078.2019.1615820.
- Brennan, K. *et al.* (2020) 'A comparison of methods for the isolation and separation of extracellular vesicles from protein and lipid particles in human serum', *Scientific Reports 2020 10:1*, 10(1), pp. 1–13. doi: 10.1038/s41598-020-57497-7.
- Burgess, T. L. and Kelly, R. B. (1987) 'Constitutive and regulated secretion of proteins', *Annual review of cell biology*, 3, pp. 243–293. doi: 10.1146/ANNUREV.CB.03.110187.001331.
- Carnino, J. M., Lee, H. and Jin, Y. (2019) 'Isolation and characterization of extracellular vesicles from Broncho-alveolar lavage fluid: a review and comparison of different methods', *Respiratory research*, 20(1). doi: 10.1186/S12931-019-1210-
- Carter, S. and Solomon, T. P. J. (2019) 'In vitro experimental models for examining the skeletal muscle cell biology of exercise'. doi: 10.1007/s00424-018-2210-4.

- Castaño, C. *et al.* (2020) 'Delivery of muscle-derived exosomal miRNAs induced by HIIT improves insulin sensitivity through down-regulation of hepatic FoxO1 in mice', *Proceedings of the National Academy of Sciences of the United States of America*, 117(48), pp. 30335–30343. doi: 10.1073/pnas.2016112117.
- Catalano, M. and O'Driscoll, L. (2019) 'Inhibiting extracellular vesicles formation and release: a review of EV inhibitors', <https://doi.org/10.1080/20013078.2019.1703244>, 9(1). doi: 10.1080/20013078.2019.1703244.
- Chaudhary, S. C. *et al.* (2018) 'Proteomic profiling of extracellular vesicles released from vascular smooth muscle cells during initiation of phosphate-induced mineralization', *Connective Tissue Research*, 59(1), pp. 55–61. doi: 10.1080/03008207.2018.1444759.
- Choi, Y. *et al.* (2015) 'Gut microbe-derived extracellular vesicles induce insulin resistance, thereby impairing glucose metabolism in skeletal muscle', *Scientific Reports*, 5(October), pp. 1–11. doi: 10.1038/srep15878.
- Colditz, G. A., Cannuscio, C. C. and Frazier, A. L. (1997) 'Physical activity and reduced risk of colon cancer: implications for prevention', *Cancer Causes & Control* 1997 8:4, 8(4), pp. 649–667. doi: 10.1023/A:1018458700185.
- Console, L., Scalise, M. and Indiveri, C. (2019) 'Exosomes in inflammation and role as biomarkers', *Clinica chimica acta; international journal of clinical chemistry*, 488, pp. 165–171. doi: 10.1016/J.CCA.2018.11.009.
- Croissant, C. *et al.* (2020) 'Annexin-A6 in Membrane Repair of Human Skeletal Muscle Cell: A Role in the Cap Subdomain', *Cells* 2020, Vol. 9, Page 1742, 9(7), p. 1742. doi: 10.3390/CELLS9071742.

- De Gasperi, R. *et al.* (2017) 'Denervation-related alterations and biological activity of miRNAs contained in exosomes released by skeletal muscle fibers', *Scientific Reports*, 7(1), pp. 1–11. doi: 10.1038/s41598-017-13105-9.
- Demonbreun, A. R. *et al.* (2016) 'An actin-dependent annexin complex mediates plasma membrane repair in muscle', *The Journal of cell biology*, 213(6), pp. 705–718. doi: 10.1083/JCB.201512022.
- Demonbreun, A. R. *et al.* (2019) 'Recombinant annexin A6 promotes membrane repair and protects against muscle injury', *The Journal of Clinical Investigation*, 129(11), pp. 4657–4670. doi: 10.1172/JCI128840.
- Denes, L. T. *et al.* (2019) 'Culturing C2C12 myotubes on micromolded gelatin hydrogels accelerates myotube maturation', *Skeletal Muscle*, 9(1), pp. 1–10. doi: 10.1186/S13395-019-0203-4/FIGURES/4.
- Denham, J. and Spencer, S. J. (2020) 'Emerging roles of extracellular vesicles in the intercellular communication for exercise-induced adaptations', *American journal of physiology. Endocrinology and metabolism*, 319(2), pp. E320–E329. doi: 10.1152/AJPENDO.00215.2020.
- Deshmukh, A. S. *et al.* (2015) 'Deep proteomics of mouse skeletal muscle enables quantitation of protein isoforms, metabolic pathways, and transcription factors', *Molecular & cellular proteomics: MCP*, 14(4), pp. 841–853. doi: 10.1074/MCP.M114.044222.
- Di, W. *et al.* (2020) 'Long-term exercise-secreted extracellular vesicles promote browning of white adipocytes by suppressing miR-191a-5p', *Life sciences*, 263. doi: 10.1016/J.LFS.2020.118464.

- Doyle, L. M. and Wang, M. Z. (2019) 'Overview of Extracellular Vesicles, Their Origin, Composition, Purpose, and Methods for Exosome Isolation and Analysis', *Cells* 2019, Vol. 8, Page 727, 8(7), p. 727. doi: 10.3390/CELLS8070727.
- Edgar, J. R. (2016) 'Q & A: What are exosomes, exactly?', *BMC Biology*, 14(1), pp. 1–7. doi: 10.1186/S12915-016-0268-Z/FIGURES/3.
- Eichner, N. Z. M., Erdbrügger, U. and Malin, S. K. (2018) 'Extracellular Vesicles: A Novel Target for Exercise-Mediated Reductions in Type 2 Diabetes and Cardiovascular Disease Risk', *Journal of Diabetes Research*, 2018. doi: 10.1155/2018/7807245.
- Jones, A. et al. (2017) 'miRNA Signatures of Insulin Resistance in Obesity', *Obesity*, 25(10), pp. 1734–1744. doi: 10.1002/OBY.21950.
- Erdbrügger, U. and Lannigan, J. (2016) 'Analytical challenges of extracellular vesicle detection: A comparison of different techniques', *Cytometry. Part A : the journal of the International Society for Analytical Cytology*, 89(2), pp. 123–134. doi: 10.1002/CYTO.A.22795.
- Estrada, A. L. et al. (2021) 'Extracellular vesicle secretion is tissue-dependent ex vivo and skeletal muscle myofiber extracellular vesicles reach the circulation in vivo.', <https://doi.org/10.1152/ajpcell.00580.2020>. doi: 10.1152/AJPCELL.00580.2020.
- Evers-Van Gogh, I. J. A. et al. (2015) 'Electric Pulse Stimulation of Myotubes as an In Vitro Exercise Model: Cell-Mediated and Non-Cell-Mediated Effects', *Scientific Reports* 2015 5:1, 5(1), pp. 1–11. doi: 10.1038/srep10944.
- Flück, M. and Hoppeler, H. (2003) 'Molecular basis of skeletal muscle plasticity--from gene to form and function', *Reviews of physiology, biochemistry and pharmacology*, 146, pp. 159–216. doi: 10.1007/S10254-002-0004-7.

- Forterre, A. *et al.* (2014) 'Proteomic analysis of C2C12 myoblast and myotube exosome-like vesicles: a new paradigm for myoblast-myotube cross talk?', *PloS one*, 9(1). doi: 10.1371/JOURNAL.PONE.0084153.
- Fox, K. R. (1999) 'The influence of physical activity on mental well-being', *Public health nutrition*, 2(3A), pp. 411–418. doi: 10.1017/S1368980099000567.
- Friedenreich, C. M. (2011) 'Physical activity and breast cancer: review of the epidemiologic evidence and biologic mechanisms', *Recent results in cancer research. Fortschritte der Krebsforschung. Progres dans les recherches sur le cancer*, 188, pp. 125–139. doi: 10.1007/978-3-642-10858-7_11.
- Frontera, W. R. and Ochala, J. (2015) 'Skeletal muscle: a brief review of structure and function', *Calcified tissue international*, 96(3), pp. 183–195. doi: 10.1007/S00223-014-9915-Y.
- Frühbeis, C. *et al.* (2015) 'Physical exercise induces rapid release of small extracellular vesicles into the circulation', *Journal of Extracellular Vesicles*, 4(1), pp. 1–11. doi: 10.3402/jev.v4.28239.
- Fujita, H., Nedachi, T. and Kanzaki, M. (2007) 'Accelerated de novo sarcomere assembly by electric pulse stimulation in C2C12 myotubes', *Experimental Cell Research*, 313(9), pp. 1853–1865. doi: 10.1016/J.YEXCR.2007.03.002.
- Fuller, O. K. *et al.* (2020) 'The Protective Effect of Exercise in Neurodegenerative Diseases: The Potential Role of Extracellular Vesicles', *Cells*, 9(10). doi: 10.3390/cells9102182.
- Fulzele, S. *et al.* (2019) 'Muscle-derived miR-34a increases with age in circulating extracellular vesicles and induces senescence of bone marrow stem cells', *Aging*, 11(6), pp. 1791–1803. doi: 10.18632/aging.101874.

- Gao, Y. *et al.* (2015) 'CD44 is a direct target of miR-199a-3p and contributes to aggressive progression in osteosarcoma', *Scientific Reports* 2015 5:1, 5(1), pp. 1–9. doi: 10.1038/srep11365.
- Garbis, S., Lubec, G. and Fountoulakis, M. (2005) 'Limitations of current proteomics technologies', *Journal of chromatography. A*, 1077(1), pp. 1–18. doi: 10.1016/J.CHROMA.2005.04.059.
- Garcia, N. A. *et al.* (2015) 'Glucose Starvation in Cardiomyocytes Enhances Exosome Secretion and Promotes Angiogenesis in Endothelial Cells', *PLOS ONE*, 10(9), p. e0138849. doi: 10.1371/JOURNAL.PONE.0138849.
- Gerke, V., Creutz, C. E. and Moss, S. E. (2005) 'Annexins: linking Ca²⁺ signalling to membrane dynamics', *Nature reviews. Molecular cell biology*, 6(6), pp. 449–461. doi: 10.1038/NRM1661.
- Geyer, P. E. *et al.* (2017) 'Revisiting biomarker discovery by plasma proteomics', *Molecular Systems Biology*, 13(9), p. 942. doi: 10.15252/MSB.20156297.
- Good, D. M. *et al.* (2007) 'Body fluid proteomics for biomarker discovery: lessons from the past hold the key to success in the future', *Journal of proteome research*, 6(12), pp. 4549–4555. doi: 10.1021/PR070529W.
- Goodison, S., Urquidi, V. and Tarin, D. (1999) 'CD44 cell adhesion molecules', *Molecular pathology: MP*, 52(4), pp. 189–196. doi: 10.1136/MP.52.4.189.
- Guescini, M. *et al.* (2010) 'C2C12 myoblasts release micro-vesicles containing mtDNA and proteins involved in signal transduction', *Experimental cell research*, 316(12), pp. 1977–1984. doi: 10.1016/J.YEXCR.2010.04.006.
- Hainaut, K. and Desmedt, J. E. (1974) 'Calcium ionophore A23187 potentiates twitch and intracellular calcium release in single muscle fibres', *Nature*, 252(5482), pp. 407–408. doi: 10.1038/252407a0.

- Hawley, J. A. *et al.* (2014) 'Integrative biology of exercise', *Cell*, 159(4), pp. 738–749. doi: 10.1016/J.CELL.2014.10.029.
- He, Q. Y. and Chiu, J. F. (2003) 'Proteomics in biomarker discovery and drug development', *Journal of cellular biochemistry*, 89(5), pp. 868–886. doi: 10.1002/JCB.10576.
- Intlekofer, K. A. and Cotman, C. W. (2013) 'Exercise counteracts declining hippocampal function in aging and Alzheimer's disease', *Neurobiology of disease*, 57, pp. 47–55. doi: 10.1016/J.NBD.2012.06.011.
- Jensen-Cody, S. O. and Potthoff, M. J. (2021) 'Hepatokines and metabolism: Deciphering communication from the liver', *Molecular metabolism*, 44. doi: 10.1016/J.MOLMET.2020.101138.
- Jeppesen, D. K. *et al.* (2019) 'Reassessment of Exosome Composition', *Cell*, 177(2), pp. 428-445.e18. doi: 10.1016/J.CELL.2019.02.029.
- Jørgensen, M. *et al.* (2013) 'Extracellular Vesicle (EV) array: Microarray capturing of exosomes and other extracellular vesicles for multiplexed phenotyping', *Journal of Extracellular Vesicles*, 2(1). doi: 10.3402/jev.v2i0.20920.
- Just, J. *et al.* (2020) 'Blood flow-restricted resistance exercise alters the surface profile, miRNA cargo and functional impact of circulating extracellular vesicles', *Scientific Reports*, 10(1), pp. 1–13. doi: 10.1038/s41598-020-62456-3.
- Kalluri, R. and LeBleu, V. S. (2020) 'The biology , function , and biomedical applications of exosomes', *Science (New York, N.Y.)*, 367(6478). doi: 10.1126/SCIENCE.AAU6977.
- Kalra, H. *et al.* (2012) 'Vesiclepedia: A Compendium for Extracellular Vesicles with Continuous Community Annotation', *PLOS Biology*, 10(12), p. e1001450. doi: 10.1371/JOURNAL.PBIO.1001450.

- Keerthikumar, S. *et al.* (2016) 'ExoCarta: A Web-Based Compendium of Exosomal Cargo', *Journal of molecular biology*, 428(4), pp. 688–692. doi: 10.1016/J.JMB.2015.09.019.
- Kemppainen, J. *et al.* (2002) 'Myocardial and skeletal muscle glucose uptake during exercise in humans', *The Journal of Physiology*, 542(2), pp. 403–412. doi: 10.1113/JPHYSIOL.2002.018135.
- Khalyfa, A. and Gozal, D. (2014) 'Exosomal miRNAs as potential biomarkers of cardiovascular risk in children', *Journal of translational medicine*, 12(1). doi: 10.1186/1479-5876-12-162.
- Kirby, T. J., Chaillou, T. and McCarthy, J. J. (2015) 'The role of microRNAs in skeletal muscle health and disease', *Frontiers in bioscience (Landmark edition)*, 20(1), pp. 37–77. doi: 10.2741/4298.
- Kobayashi, Y. *et al.* (2021) 'Protein Composition of Circulating Extracellular Vesicles Immediately Changed by Particular Short Time of High-Intensity Interval Training Exercise', *Frontiers in physiology*, 12. doi: 10.3389/FPHYS.2021.693007.
- Koutsoulidou, A. *et al.* (2015) 'Elevated muscle-specific miRNAs in serum of myotonic dystrophy patients relate to muscle disease progress', *PLoS ONE*, 10(4), pp. 1–20. doi: 10.1371/journal.pone.0125341.
- Kowal, J. *et al.* (2016) 'Proteomic comparison defines novel markers to characterize heterogeneous populations of extracellular vesicle subtypes', *Proceedings of the National Academy of Sciences of the United States of America*, 113(8), pp. E968–E977. doi: 10.1073/PNAS.1521230113/-/DCSUPPLEMENTAL.
- Kugeratski, F. G. *et al.* (2021) 'Quantitative proteomics identifies the core proteome of exosomes with syntenin-1 as the highest abundant protein and a putative universal

biomarker', *Nature cell biology*, 23(6), pp. 631–641. doi: 10.1038/S41556-021-00693-Y.

- Lambernd, S. *et al.* (2012) 'Contractile activity of human skeletal muscle cells prevents insulin resistance by inhibiting pro-inflammatory signalling pathways', *Diabetologia*, 55(4), pp. 1128–1139. doi: 10.1007/S00125-012-2454-Z/FIGURES/8.
- Langen, R. C. 1 *et al.* (no date) 'ENHANCED MYOGENIC DIFFERENTIATION BY EXTRACELLULAR MATRIX IS REGULATED AT THE EARLY STAGES OF MYOGENESIS', *In Vitro Cell. Dev. Biol.-Animal*, 39, pp. 163–169.
- Lässer, C., Jang, S. C. and Lötvall, J. (2018) 'Subpopulations of extracellular vesicles and their therapeutic potential', *Molecular Aspects of Medicine*, 60, pp. 1–14. doi: 10.1016/J.MAM.2018.02.002.
- Laurens, C. *et al.* (2020) 'Growth and differentiation factor 15 is secreted by skeletal muscle during exercise and promotes lipolysis in humans', *JCI Insight*, 5(6). doi: 10.1172/JCI.INSIGHT.131870.
- Lautaoja, J. H. *et al.* (2021) 'Higher glucose availability augments the metabolic responses of the c2c12 myotubes to exercise-like electrical pulse stimulation', *American Journal of Physiology - Endocrinology and Metabolism*, 321(2), pp. E229–E245. doi: 10.1152/AJPENDO.00133.2021/ASSET/IMAGES/MEDIUM/E-00133-2021R01.PNG.
- Le Bihan, M. C. *et al.* (2012) 'In-depth analysis of the secretome identifies three major independent secretory pathways in differentiating human myoblasts', *Journal of Proteomics*, 77, pp. 344–356. doi: 10.1016/J.JPROT.2012.09.008.
- Leal, L. G., Lopes, M. A. and Batista, M. L. (2018) 'Physical exercise-induced myokines and muscle-adipose tissue crosstalk: A review of current knowledge and the

implications for health and metabolic diseases', *Frontiers in Physiology*, 9(SEP), pp. 1–17. doi: 10.3389/fphys.2018.01307.

- Lehrich, B. M., Liang, Y. and Fiandaca, M. S. (2021) 'Foetal bovine serum influence on in vitro extracellular vesicle analyses', *Journal of Extracellular Vesicles*, 10(3). doi: 10.1002/jev2.12061.
- Leng, Y. *et al.* (2019) 'Hyaluronic acid, CD44 and RHAMM regulate myoblast behavior during embryogenesis', *Matrix biology: journal of the International Society for Matrix Biology*, 78–79, pp. 236–254. doi: 10.1016/J.MATBIO.2018.08.008.
- Lin, J. *et al.* (2015) 'Exosomes: Novel Biomarkers for Clinical Diagnosis', *Scientific World Journal*, 2015. doi: 10.1155/2015/657086.
- Lisitsa, A. *et al.* (2014) 'Profiling proteoforms: promising follow-up of proteomics for biomarker discovery', <http://dx.doi.org/10.1586/14789450.2014.878652>, 11(1), pp. 121–129. doi: 10.1586/14789450.2014.878652.
- Liu, T. *et al.* (2018) 'CRISPR-Cas9-Mediated Silencing of CD44 in Human Highly Metastatic Osteosarcoma Cells', *Cellular physiology and biochemistry: international journal of experimental cellular physiology, biochemistry, and pharmacology*, 46(3), pp. 1218–1230. doi: 10.1159/000489072.
- M. Gleser, D. H. Horstman and R. P. Mello (1974) 'The effect on Vo2 max of adding arm work to maximal leg work', *Medicine and Science in Sport*, 6(2), pp. 7–104. Available at: https://www.researchgate.net/publication/18703981_The_effect_on_Vo2_max_of_adding_arm_work_to_maximal_leg_work (Accessed: 15 January 2022).
- Ma, C. *et al.* (2018) 'Moderate Exercise Enhances Endothelial Progenitor Cell Exosomes Release and Function.', *Medicine and Science in Sports and Exercise*, 50(10), pp. 2024–2032. doi: 10.1249/MSS.0000000000001672.

- Magliulo, L. *et al.* (2021) 'The wonder exerkines—novel insights: a critical state-of-the-art review', *Molecular and Cellular Biochemistry*, 477(1), pp. 105–113. doi: 10.1007/S11010-021-04264-5/FIGURES/2.
- Mallick, R. L. *et al.* (2015) 'Prion protein fragment (106-126) induces prothrombotic state by raising platelet intracellular calcium and microparticle release', *Cell calcium*, 57(4), pp. 300–311. doi: 10.1016/J.CECA.2015.02.002.
- Mann, M. (2008) 'Can Proteomics Retire the Western Blot?', *Journal of Proteome Research*, 7(8), p. 3065. doi: 10.1021/PR800463V.
- Martínez, M. C. and Andriantsitohaina, R. (2017) 'Extracellular vesicles in metabolic syndrome', *Circulation Research*, 120(10), pp. 1674–1686. doi: 10.1161/CIRCRESAHA.117.309419.
- Mayr, L. *et al.* (2017) 'CD44 drives aggressiveness and chemoresistance of a metastatic human osteosarcoma xenograft model', *Oncotarget*, 8(69), p. 114095. doi: 10.18632/ONCOTARGET.23125.
- Meligy, F. Y. *et al.* (2012) 'The efficiency of in vitro isolation and myogenic differentiation of MSCs derived from adipose connective tissue, bone marrow, and skeletal muscle tissue', *In Vitro Cellular and Developmental Biology - Animal*, 48(4), pp. 203–215. doi: 10.1007/S11626-012-9488-X/FIGURES/8.
- Millet, G. P., Vleck, V. E. and Bentley, D. J. (2009) 'Physiological differences between cycling and running: lessons from triathletes', *Sports medicine (Auckland, N.Z.)*, 39(3), pp. 179–206. doi: 10.2165/00007256-200939030-00002.
- Moreira-Costa, L. *et al.* (2021) 'Exosome-Derived Mediators as Potential Biomarkers for Cardiovascular Diseases: A Network Approach', *Proteomes*, 9(1), pp. 1–29. doi: 10.3390/PROTEOMES9010008.

- Mulcahy, L. A., Pink, R. C. and Carter, D. R. F. (2014) 'Routes and mechanisms of extracellular vesicle uptake', *Journal of extracellular vesicles*, 3(1). doi: 10.3402/JEV.V3.24641.
- Mylona, E. *et al.* (2006) 'CD44 regulates myoblast migration and differentiation', *Journal of Cellular Physiology*, 209(2), pp. 314–321. doi: 10.1002/JCP.20724.
- Mytidou, C. *et al.* (2021) 'Muscle-derived exosomes encapsulate myomiRs and are involved in local skeletal muscle tissue communication', *FASEB journal: official publication of the Federation of American Societies for Experimental Biology*, 35(2). doi: 10.1096/FJ.201902468RR.
- Needham, E. J. *et al.* (2019) 'Phosphoproteomics of Acute Cell Stressors Targeting Exercise Signaling Networks Reveal Drug Interactions Regulating Protein Secretion', *Cell Reports*, 29(6), pp. 1524-1538.e6. doi: 10.1016/j.celrep.2019.10.001.
- Nickel, W. and Seedorf, M. (2008) 'Unconventional mechanisms of protein transport to the cell surface of eukaryotic cells', *Annual review of cell and developmental biology*, 24, pp. 287–308. doi: 10.1146/ANNUREV.CELLBIO.24.110707.175320.
- Nie, Y. *et al.* (2019) 'Skeletal muscle-derived exosomes regulate endothelial cell functions via reactive oxygen species-activated nuclear factor-κB signalling', *Experimental Physiology*, 104(8), pp. 1262–1273. doi: 10.1113/EP087396.
- Oliveira, G. P. *et al.* (2018) 'Effects of acute aerobic exercise on rats serum extracellular vesicles diameter, concentration and small RNAs content', *Frontiers in Physiology*, 9(MAY), p. 532. doi: 10.3389/FPHYS.2018.00532/BIBTEX.
- Olsson, K. *et al.* (2015) 'Intracellular Ca²⁺-handling differs markedly between intact human muscle fibers and myotubes', *Skeletal Muscle*, 5(1), pp. 1–14. doi: 10.1186/S13395-015-0050-X/FIGURES/6.

- Pavani, K. C. *et al.* (2019) 'Isolation and Characterization of Functionally Active Extracellular Vesicles from Culture Medium Conditioned by Bovine Embryos In Vitro', *International Journal of Molecular Sciences*, 20(1). doi: 10.3390/IJMS20010038.
- Pečan, P. *et al.* (2020) 'Calcium Ionophore-Induced Extracellular Vesicles Mediate Cytoprotection against Simulated Ischemia/Reperfusion Injury in Cardiomyocyte-Derived Cell Lines by Inducing Heme Oxygenase 1', *International Journal of Molecular Sciences* 2020, Vol. 21, Page 7687, 21(20), p. 7687. doi: 10.3390/IJMS21207687.
- Pegtel, D. M. and Gould, S. J. (2019) 'Exosomes', *The Annual Reviews of Biochemistry*. Kalluri, R. and LeBleu, V. S. (2020) 'The biology, function, and biomedical applications of exosomes', *Science*, 367(6478). doi: 10.1126/science.aau6977.
- Petersen, T. N. *et al.* (2011) 'SignalP 4.0: discriminating signal peptides from transmembrane regions', *Nature Methods* 2011 8:10, 8(10), pp. 785–786. doi: 10.1038/nmeth.1701.
- Properzi, F., Logozzi, M. and Fais, S. (2013) 'Exosomes: the future of biomarkers in medicine', *Biomarkers in medicine*, 7(5), pp. 769–778. doi: 10.2217/BMM.13.63.
- Rak, J. (2013) 'Extracellular Vesicles – Biomarkers and Effectors of the Cellular Interactome in Cancer', *Frontiers in Pharmacology*, 4. doi: 10.3389/FPHAR.2013.00021.
- Rani, A. *et al.* (2017) 'miRNA in Circulating Microvesicles as Biomarkers for Age-Related Cognitive Decline', *Frontiers in Aging Neuroscience*, 9(OCT). doi: 10.3389/FNAGI.2017.00323.
- Raposo, G. and Stoorvogel, W. (2013) 'Extracellular vesicles: Exosomes, microvesicles, and friends', *Journal of Cell Biology*, 200(4), pp. 373–383. doi: 10.1083/jcb.201211138.

- Reybrouck, T., Heigenhauser, G. F. and Faulkner, J. A. (1975) 'Limitations to maximum oxygen uptake in arms, leg, and combined arm-leg ergometry', *https://doi.org/10.1152/jappl.1975.38.5.774*, 38(5), pp. 774–779. doi: 10.1152/JAPPL.1975.38.5.774.
- Rigamonti, A. E. *et al.* (2020) 'Effects of an acute bout of exercise on circulating extracellular vesicles: tissue-, sex-, and BMI-related differences', *International journal of obesity (2005)*, 44(5), pp. 1108–1118. doi: 10.1038/S41366-019-0460-7.
- Romacho, T. *et al.* (2014) 'Adipose tissue and its role in organ crosstalk', *Acta Physiologica*, 210(4), pp. 733–753. doi: 10.1111/APHA.12246.
- Romancino, D. P. *et al.* (2013) 'Identification and characterization of the nano-sized vesicles released by muscle cells', *FEBS letters*, 587(9), pp. 1379–1384. doi: 10.1016/J.FEBSLET.2013.03.012.
- Savina, A. *et al.* (2003) 'Exosome release is regulated by a calcium-dependent mechanism in K562 cells', *The Journal of biological chemistry*, 278(22), pp. 20083–20090. doi: 10.1074/JBC.M301642200.
- Scheler, M. *et al.* (2013) 'Cytokine response of primary human myotubes in an in vitro exercise model', *American Journal of Physiology - Cell Physiology*, 305(8), pp. 877–886. doi: 10.1152/ajpcell.00043.2013.
- Scimeca, M. *et al.* (2015) 'Satellite Cells CD44 Positive Drive Muscle Regeneration in Osteoarthritis Patients', *Stem Cells International*, 2015. doi: 10.1155/2015/469459.
- Senbanjo, L. T. and Chellaiah, M. A. (2017) 'CD44: A Multifunctional Cell Surface Adhesion Receptor Is a Regulator of Progression and Metastasis of Cancer Cells', *Frontiers in cell and developmental biology*, 5(MAR). doi: 10.3389/FCELL.2017.00018.

- Severinsen, M. C. K. and Pedersen, B. K. (2020) 'Muscle-Organ Crosstalk: The Emerging Roles of Myokines', *Endocrine reviews*, 41(4), pp. 594–609. doi: 10.1210/ENDREV/BNAA016.
- Shelke, G. V. *et al.* (2014) 'Importance of exosome depletion protocols to eliminate functional and RNA-containing extracellular vesicles from fetal bovine serum', *Journal of extracellular vesicles*, 3(1). doi: 10.3402/JEV.V3.24783.
- Siqueira, I. R., Palazzo, R. P. and Cechinel, L. R. (2021) 'Circulating extracellular vesicles delivering beneficial cargo as key players in exercise effects', *Free Radical Biology and Medicine*, 172, pp. 273–285. doi: 10.1016/J.FREERADBIOMED.2021.06.007.
- Soung, Y. H. *et al.* (2017) 'Exosomes in Cancer Diagnostics', *Cancers*, 9(1). doi: 10.3390/CANCERS9010008.
- Tada, H. *et al.* (2000) 'Myocardial Glucose Uptake Is Regulated by Nitric Oxide via Endothelial Nitric Oxide Synthase in Langendorff Mouse Heart', *Circulation Research*, 86(3), pp. 270–274. doi: 10.1161/01.RES.86.3.270.
- Takafuji, Y. *et al.* (2020) 'Extracellular vesicles secreted from mouse muscle cells suppress osteoclast formation: Roles of mitochondrial energy metabolism', *Bone*, 134(February), p. 115298. doi: 10.1016/j.bone.2020.115298.
- Tambor, V. *et al.* (2010) 'Application of proteomics in biomarker discovery: A primer for the clinician', *Physiological Research*, 59(4), pp. 471–497. doi: 10.33549/PHYSIOLRES.931758.
- Tarakci, H. and Berger, J. (2016) 'The sarcoglycan complex in skeletal muscle', *Frontiers in bioscience (Landmark edition)*, 21(4), pp. 744–756. doi: 10.2741/4418.

- Taylor, J. *et al.* (2020) 'Ca²⁺ mediates extracellular vesicle biogenesis through alternate pathways in malignancy', *Journal of Extracellular Vesicles*, 9(1). doi: 10.1080/20013078.2020.1734326.
- Théry, C. *et al.* (1999) 'Molecular characterization of dendritic cell-derived exosomes: Selective accumulation of the heat shock protein hsc73', *Journal of Cell Biology*, 147(3), pp. 599–610. doi: 10.1083/jcb.147.3.599.
- Trovato, E., Di Felice, V. and Barone, R. (2019) 'Extracellular vesicles: Delivery vehicles of myokines', *Frontiers in Physiology*, 10(MAY), p. 522. doi: 10.3389/FPHYS.2019.00522/BIBTEX.
- Tyanova, S. *et al.* (2016) 'The Perseus computational platform for comprehensive analysis of (prote)omics data', *Nature Methods* 2016 13:9, 13(9), pp. 731–740. doi: 10.1038/nmeth.3901.
- Uhlén, M. *et al.* (2015) 'Proteomics. Tissue-based map of the human proteome', *Science (New York, N.Y.)*, 347(6220). doi: 10.1126/SCIENCE.1260419.
- van der Vlist, E. J. *et al.* (2012) 'CD4(+) T cell activation promotes the differential release of distinct populations of nanosized vesicles', *Journal of extracellular vesicles*, 1(1). doi: 10.3402/JEV.V1I0.18364.
- Vanderboom, P. M. *et al.* (2021) 'A size-exclusion-based approach for purifying extracellular vesicles from human plasma', *Cell Reports Methods*, 1. doi: 10.1016/j.crmeth.2021.100055.
- Vechetti, I. J. *et al.* (2021) 'The role of extracellular vesicles in skeletal muscle and systematic adaptation to exercise', *Journal of Physiology*, 599(3), pp. 845–861. doi: 10.1113/JP278929.

- Veenstra, T. D. (2007) 'Global and targeted quantitative proteomics for biomarker discovery', *Journal of Chromatography B*, 847(1), pp. 3–11. doi: 10.1016/J.JCHROMB.2006.09.004.
- Vion, A. C. *et al.* (2013) 'Shear stress regulates endothelial microparticle release', *Circulation research*, 112(10), pp. 1323–1333. doi: 10.1161/CIRCRESAHA.112.300818.
- Warburton, D. E. R., Nicol, C. W. and Bredin, S. S. D. (2006) 'Health benefits of physical activity: the evidence', *CMAJ: Canadian Medical Association Journal*, 174(6), p. 801. doi: 10.1503/CMAJ.051351.
- Wei, Z. *et al.* (2016) 'Fetal Bovine Serum RNA Interferes with the Cell Culture derived Extracellular RNA', *Scientific Reports 2016 6:1*, 6(1), pp. 1–6. doi: 10.1038/srep31175.
- Whitham, M. and Febbraio, M. A. (2016) 'The ever-expanding myokinome: discovery challenges and therapeutic implications', *Nature reviews. Drug discovery*, 15(10), pp. 719–729. doi: 10.1038/NRD.2016.153.
- Whitham, M. and Febbraio, M. A. (2019) 'Redefining Tissue Crosstalk via Shotgun Proteomic Analyses of Plasma Extracellular Vesicles', *Proteomics*, 19(1–2). doi: 10.1002/pmic.201800154.
- Whitham, M. *et al.* (2018) 'Extracellular Vesicles Provide a Means for Tissue Crosstalk during Exercise'. doi: 10.1016/j.cmet.2017.12.001.
- Wiklander, O. P. B. *et al.* (2015) 'Extracellular vesicle in vivo biodistribution is determined by cell source, route of administration and targeting', *Journal of extracellular vesicles*, 4(2015), pp. 1–13. doi: 10.3402/JEV.V4.26316.
- Witwer, K. W. *et al.* (2013) 'Standardization of sample collection, isolation and analysis methods in extracellular vesicle research', *Journal of Extracellular Vesicles*, 2(1). doi: 10.3402/JEV.V2I0.20360.

- Wong, C. H. and Chen, Y. C. (2019) 'Clinical significance of exosomes as potential biomarkers in cancer', *World Journal of Clinical Cases*, 7(2), p. 171. doi: 10.12998/WJCC.V7.I2.171.
- Wu, Y., Huang, Q. and Bu, S. (2020) 'Cross talk between exosomes and pancreatic β -cells in diabetes', *Archives of Physiology and Biochemistry*, 3455. doi: 10.1080/13813455.2020.1760303.
- Z.György, B. *et al.* (2011) 'Membrane vesicles, current state-of-the-art: emerging role of extracellular vesicles', *Cellular and molecular life sciences: CMLS*, 68(16), pp. 2667–2688. doi: 10.1007/S00018-011-0689-3.
- Zamani, P. *et al.* (2019) 'The therapeutic and diagnostic role of exosomes in cardiovascular diseases', *Trends in Cardiovascular Medicine*, 29(6), pp. 313–323. doi: 10.1016/J.TCM.2018.10.010.
- Zhang, J. *et al.* (2019) 'CD44+/CD24+-Expressing Cervical Cancer Cells and Radioresistant Cervical Cancer Cells Exhibit Cancer Stem Cell Characteristics', *Gynecologic and obstetric investigation*, 84(2), pp. 174–182. doi: 10.1159/000493129.
- Zhou, H. *et al.* (2008) 'Urinary exosomal transcription factors, a new class of biomarkers for renal disease', *Kidney International*, 74(5), pp. 613–621. doi: 10.1038/KI.2008.206.

6. Supplementary

Figure S1.

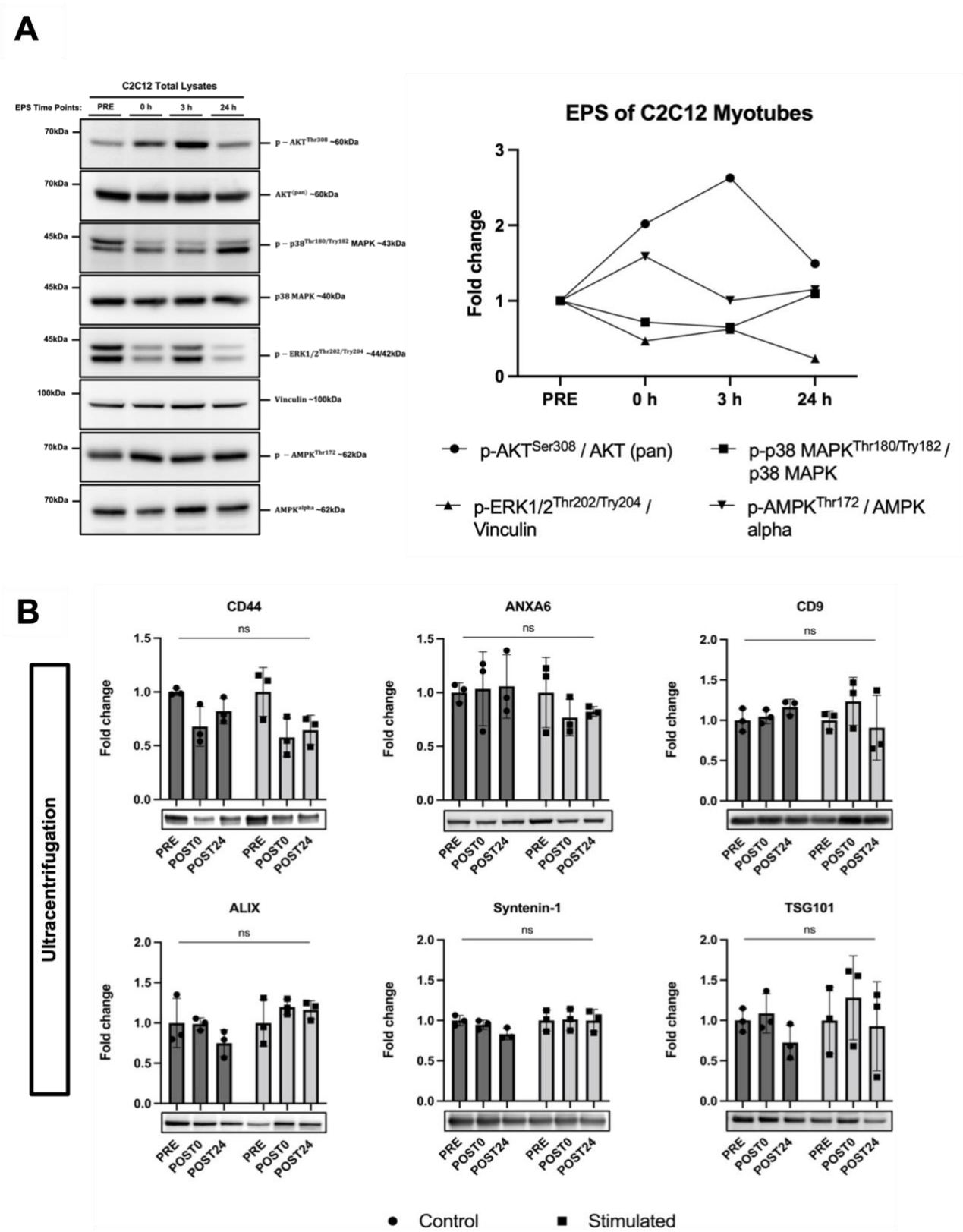


Figure S1. Electrical pulse stimulation (EPS) does not alter the abundance of sEVs expressing CD44 or ANXA6 as well as canonical markers CD9, ALIX, Syntenin-1 and TSG101. (A) EPS mediates phosphorylation of proteins involved in contraction and energy signaling. Conditioned media from C2C12 subject to EPS was collected before (PRE), immediately after (0 h) as well as at 3 (3 h) and 24 (24 h) hours into recovery. Samples were subject to SDS-PAGE and immunoblotting for target markers comparing each time point. Representative images are shown. Quantitative data represents phosphorylation over total protein and is shown as fold change relative to the PRE of each group from $n = 1$ (2 technical replicate from each conditioned at each time point). (B) EPS of C2C12 myotubes does not alter the abundance of sEVs expressing CD44, ANXA6 or markers of sEVs. sEVs were isolated by ultracentrifugation (UC) from conditioned media of C2C12 myotubes subject to 24 hours of either EPS or Control conditions. Conditioned media was collected before (PRE), immediately after (POST0) and after 24 hours of recovery (POST24). EV lysates were subject to SDS-PAGE and immunoblotting for specific antibodies. Quantitative data from immunoblots was analyzed by two-way ANOVA from $n = 3$ (6 technical replicates from each condition at each time point per n). Representative images are shown below each quantification. Percentage (%) change between time points for cell lysates was produced from difference in raw data; for sEV lysates, percentage (%) change was calculated based on fold change. Data is presented as fold change relative to the PRE of each condition. Individual data points including the mean \pm SD are shown; * = $P < 0.05$, ** = $P < 0.01$, *** = $P < 0.001$, **** = $P < 0.0001$.

Figure S2.

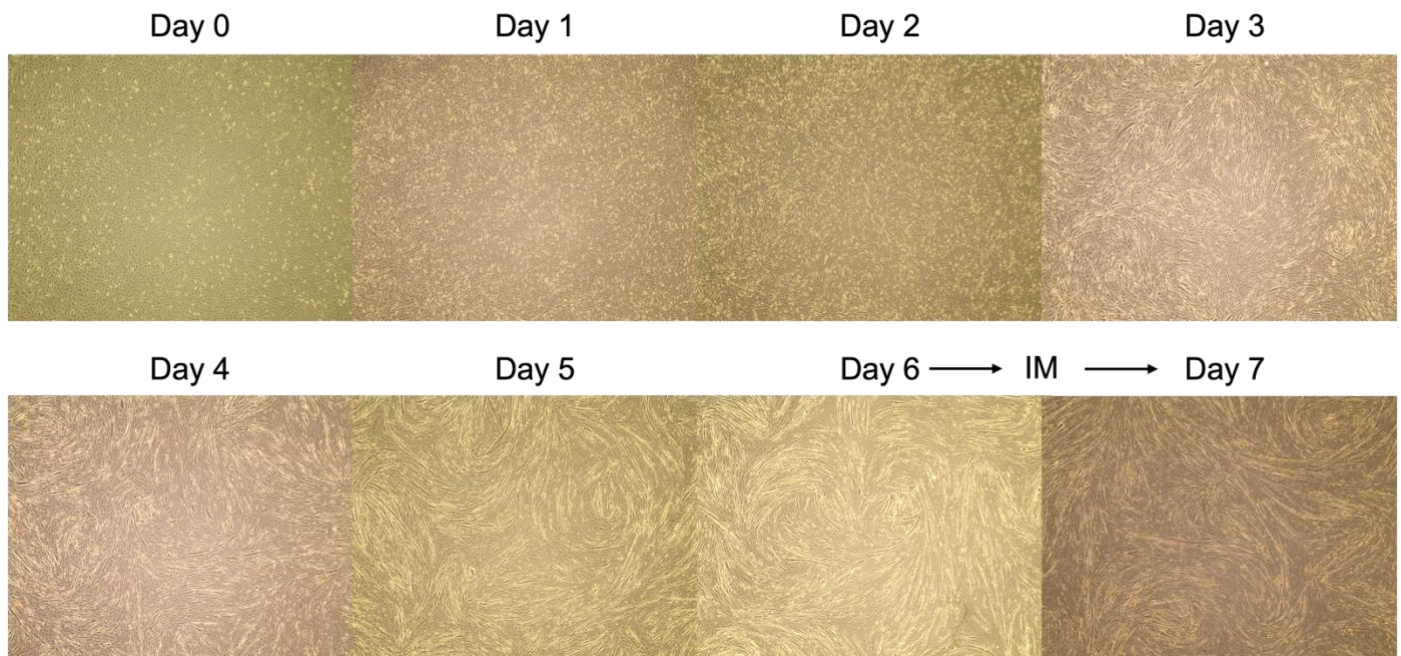


Figure S2. Ionomycin (IM) treatment does not alter C2C12 myotube structure. Images were taken daily from the start of myoblast differentiation (Day 0) to fully differentiated myotubes (Day 6) as well as after 24 hours of IM treatment (Day 7) to determine whether IM treatment influenced myotube structure and cell death.

Figure S3.

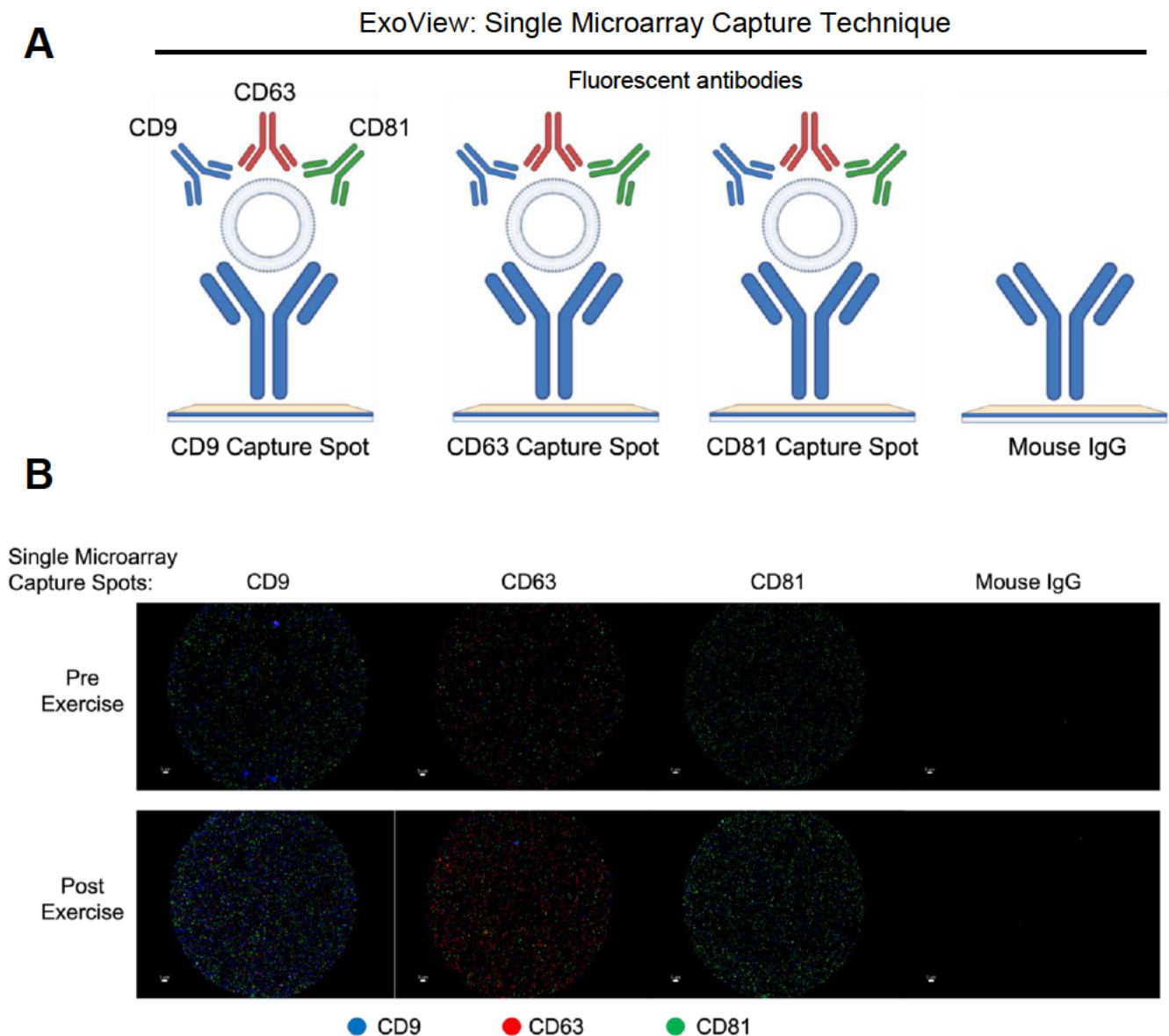


Figure S3. ExoView analysis by single microarray capture spots for CD9+, CD63+ and CD81+ enables visualization of individual CD9+, CD63+ and CD81+ vesicles, highlighting the increase pre-post exercise. (A) Schematic of ExoView isolation of tetraspanin positive sEVs to each capture spot, allowing for the fluorescence of individual sEVs based on the expression of the three tetraspanins highlighted by secondary antibody binding. (B) Visualization of pre and post exercise of individual vesicles positive for CD9, CD63 or CD81 by secondary fluorescent antibodies. CD9 = blue, CD63 = red, CD81 = green.

TABLE S1: List of 39 proteins generated by the re-analysis of significantly upregulated proteins secreted from human primary myotubes into conditioned media after 24 hours EPS (Laurens et al., 2020)

Significant	LOG(P-value)	Difference	Protein names	Gene names	Mol. weight [kDa]
+	3.049375	1.046075	Phosphoribosyl pyrophosphate synthase-associated protein 2	PRPSAP2	40.883
+	2.904611	0.567254	Ubiquitin-conjugating enzyme E2 L3	UBE2L3	17.861
+	2.679013	1.047853	X-ray repair cross-complementing protein 6	XRCC6	69.842
+	2.541529	0.798304	Catenin beta-1	CTNNB1	77.206
+	2.217356	2.914467	Extracellular sulfatase Sulf-1	DKFZp686F13142;SULF1	101.05
+	2.421601	1.202231	Annexin A6;Annexin	ANXA6	75.872
+	2.26993	0.864117	Transforming growth factor-beta-induced protein ig-h3	TGFB1	74.68
+	3.444108	2.965472	Endosialin	CD248	71.263
+	3.077863	0.911694	BTB/POZ domain-containing protein KCTD12	KCTD12	35.73
+	2.919441	1.015818	Casein kinase II subunit alpha;Casein kinase II subunit alpha 3	CSNK2A1;CSNK2A3	41.79
+	2.951146	2.061325	Coiled-coil domain-containing protein 80	okuribin;CCDC80	108.08
+	2.913664	1.396166	CD44 antigen	CD44	22.683
+	1.845141	1.386194	Neurolysin, mitochondrial	NLN	80.677
+	2.850299	2.334583	Sushi domain-containing protein 5	SUSD5	67.946
+	3.528952	8.917846			37.908
+	3.16635	1.637378	Semaphorin-3C	SEMA3C	87.168
+	2.315064	0.904111	Plexin domain-containing protein 2	PLXDC2	58.183
+	2.357364	1.161329	Sodium/potassium-transporting ATPase subunit alpha-1;Sodium/potassium-transporting ATPase subunit alpha-3	ATP1A1;ATP1A3	112.44
+	2.326131	1.713848	Vesicle-fusing ATPase	NSF	82.091
+	2.708581	0.867895			78.831
+	2.478084	1.949314	Fibulin-2	FBLN2;DKFZp586A1519	129.38
+	3.014416	1.897133	Midkine	MDK	14.374
+	2.597992	0.708879	Laminin subunit alpha-5	LAMA5	399.73
+	4.762244	3.678153	Core histone macro-H2A.1;Histone H2A	H2AFY	39.617
+	2.528475	0.724171	Gelsolin	GSN	85.696
+	2.451313	1.468411	Thrombospondin-1	THBS1	129.38
+	2.337696	2.164835	Myosin-8	MYH8	222.76
+	2.811407	2.808917	Metalloproteinase inhibitor 3	TIMP3	24.145
+	2.988213	3.001915	Tissue factor pathway inhibitor 2	TFPI2	19.365
+	2.423416	0.751192	Transitional endoplasmic reticulum ATPase	HEL-S-70;VCP;DKFZp434K0126	89.321

+	2.27116	0.770498	SUMO-conjugating enzyme UBC9	UBE2I	18.007
+	2.039877	1.046908	Histone H3.1	HIST1H3A	15.404
+	2.169304	0.964461	Transgelin	TAGLN	22.611
+	1.970877	1.98831	Collagen alpha-1(XVI) chain	COL16A1	157.75
+	1.873237	1.81211	Lysyl oxidase homolog 1	LOXL1	63.109
+	2.826174	2.03831	Connective tissue growth factor	CTGF	38.069
+	3.030684	1.800984	Growth/differentiation factor 15	GDF15	34.14
+	2.691698	1.136236	Interleukin-17B	IL17B	20.437
+	2.432632	1.354745	FACT complex subunit SPT16	SUPT16H	119.91

Table S2. List of 120 proteins generated by the re-analysis of significantly upregulated proteins in EVs isolated from human arterial plasma post exercise (Whitham et al., 2018)

Significant	LOG(P-value)	Difference	Protein names	Gene names	Mol. weight [kDa]
+	2.4143647 75	1.745003 418		PECAM1	82.521
+	2.2994178 69	1.897396 279	Myristoylated alanine-rich C-kinase substrate	MARCKS	31.595
+	4.3261391 89	2.828856 999	Low affinity immunoglobulin gamma Fc region receptor III-B	FCGR3B	24.421
+	2.7127671 48	2.141320 623	Protein-tyrosine-phosphatase; Receptor-type tyrosine-protein phosphatase C	PTPRC	131.13
+	2.8660935 27	2.140047 562	Heat shock 70 kDa protein 1B; Heat shock 70 kDa protein 1A	HSPA1B; HSPA1A	70.108
+	2.1999386 46	1.975272 716	HLA class II histocompatibility antigen, DR alpha chain	HLA-DRA	28.621
+	4.1883581 75	3.870778 848	Histone H2A type 1-J; Histone H2A type 1-H; Histone H2A.J; Histone H2A type 1-C; Histone H2A type 3; Histone H2A type 1-D; Histone H2A type 1; Histone H2A type 1-B/E; Histone H2A; Histone H2AX; Histone H2A type 1-A	HIST1H2AJ; HIST1H2AH; HIST2AFJ; HIST1H2AC; HIST3H2A; HIST1H2AD; HIST1H2AG; HIST1H2AB; H2AFX; HIST1H2AA	18.481
+	2.9832295 09	1.357787 511	HLA class I histocompatibility antigen, A-2 alpha chain	HLA-A	40.79
+	3.8133818 78	3.282273 215	Histone H2B; Histone H2B type 1-M; Histone H2B type 1-N; Histone H2B type 1-H; Histone H2B type 2-F; Histone H2B type 1-C/E/F/G/I; Histone H2B type 1-D; Histone H2B type 1-K; Histone H2B type 1-L; Histone H2B type F-S	HIST1H2BI; HIST1H2BN; HIST1H2BM; HIST1H2BH; HIST2H2BF; HIST1H2BC; HIST1H2BD; HIST1H2BK; HIST1H2BL; H2BFS	13.906
+	2.1856712 67	1.102528 509	Ubiquitin-60S ribosomal protein L40; Ubiquitin-60S ribosomal protein L40; Ubiquitin-40S ribosomal protein	UBB; RPS27A; UBC; UBA52	10.469

			S27a;Ubiquitin;40S ribosomal protein S27a;Polyubiquitin-B;Ubiquitin;Polyubiquitin-C;Ubiquitin		
+	2.5689719 18	2.605394 042	Ezrin	EZR	69.371
+	3.5649049 66	3.987939 808	Lactotransferrin;Lactoferricin-H;Kaliocin-1;Lactoferritin-A;Lactoferritin-B;Lactoferritin-C	LTF	77.969
+	2.1436277 98	1.090193 651	CD59 glycoprotein	CD59	11.985
+	2.7413220 52	1.787849 228	Cyclin-dependent kinase 2	CDK2	39.178
+	2.6147845 13	1.066754 434	Calmodulin	CALM2;CALM1	20.762
+	1.9907289 79	1.082651 491	Chloride intracellular channel protein 1	CLIC1	26.922
+	2.0505752 65	1.916881 801	Actin-related protein 2/3 complex subunit 2	ARPC2	34.333
+	2.2838623 71	2.303771 854	WD repeat-containing protein 1	WDR1	66.193
+	2.1382204 46	0.998323 676	SH3 domain-binding glutamic acid-rich-like protein	SH3BGRL	12.774
+	2.2212903 86	1.422532 202	Syntaxin-11	STX11	33.195
+	3.8222227 03	2.044920 945	Protein XRP2	RP2	39.641
+	1.7334748 27	2.665750 065	Flotillin-1	FLOT1	47.355
+	2.2421005 77	1.795217 322	L-lactate dehydrogenase A chain	LDHA	36.688
+	3.1164719	1.593709 155	Superoxide dismutase [Cu-Zn]	SOD1	15.936
+	2.0289832 75	2.695692 951	Coagulation factor VIII;Factor VIIIa heavy chain, 200 kDa isoform;Factor VIIIa heavy chain, 92 kDa isoform;Factor VIII B chain;Factor VIIIa light chain	F8	267.01
+	2.7043062 03	1.644041 76	Phosphoglycerate kinase 1	PGK1	44.614
+	1.9944131 3	1.132285 994	GTPase NRas	NRAS	21.229
+	2.2059295 3	1.902580 213	Fructose-bisphosphate aldolase A;Fructose-bisphosphate aldolase	ALDOA	39.42
+	3.5985268 38	3.554304 194	Annexin A1	ANXA1	38.714
+	2.8263883 28	2.157235 534	HLA class II histocompatibility antigen, DRB1-1 beta chain	HLA-DRB1	29.914
+	2.3192822 03	1.248021 257	Glyceraldehyde-3-phosphate dehydrogenase	GAPDH	36.053
+	2.6285929 88	1.399235 494	Heat shock protein beta-1	HSPB1	22.782
+	3.4554497 87	2.937753 933	Cytochrome b-245 heavy chain	CYBB	65.335
+	2.8982919 17	2.006668 742	Guanine nucleotide-binding protein G(i) subunit alpha-2	GNAI2	40.45

+	2.7735091 2	2.455851 313	Sodium/potassium-transporting ATPase subunit alpha-1	ATP1A1	112.89
+	4.7465084 8	2.671084 505	Integrin beta-2	ITGB2	84.781
+	3.9363876 74	2.389510 003	Protein S100-A8;Protein S100-A8, N-terminally processed	S100A8	10.834
+	2.6757924 74	1.581163 558	Integrin beta-1	ITGB1	88.414
+	4.6186003 68	2.125497 574	Protein S100-A9	S100A9	13.242
+	2.5518866 48	1.136902 736	Protein S100-A6;Protein S100	S100A6	10.18
+	2.8403028 23	1.313226 194	Alpha-enolase	ENO1	47.168
+	2.6470669 71	2.354445 731	Protein disulfide-isomerase	P4HB	57.116
+	2.6162072 42	2.052769 815	Annexin A2;Annexin;Putative annexin A2-like protein	ANXA2;ANXA2P2	38.604
+	2.6195177 94	1.111739 534	Profilin-1	PFN1	15.054
+	2.4197625 63	2.014823 97	Tyrosine-protein kinase Lyn	LYN	58.573
+	3.2541367 85	2.542861 419	Annexin A6;Annexin	ANXA6	75.872
+	2.2541290 07	2.217019 996	Vimentin	VIM	53.651
+	3.3698791 98	2.727272 256	Annexin A5;Annexin	ANXA5	35.936
+	2.5795907 99	1.496621 76	Glutathione S-transferase P	GSTP1	23.356
+	2.7698021 18	1.439739 859	HLA class I histocompatibility antigen, A-69 alpha chain	HLA-A	40.976
+	2.8189352 52	1.177151 744	Thioredoxin	TXN	11.737
+	2.2093464 83	0.893748 65	Heat shock cognate 71 kDa protein	HSPA8	70.897
+	3.6694560 13	4.588909 884	Integrin alpha-M	ITGAM	127.18
+	3.6217741 25	1.792840 969	Ras-related protein Ral-A	RALA	23.567
+	3.0560780 85	2.351793 805	Ras-related protein Ral-B	RALB	23.408
+	2.5908708 74	2.217760 978	Plastin-2	LCP1	70.288
+	2.2371840 88	1.494158 59	CD99 antigen	CD99	18.848
+	2.0639117 68	1.551240 453	Pyruvate kinase PKM;Pyruvate kinase	PKM	57.936
+	2.4302902 38	1.664662 055	Ras-related C3 botulinum toxin substrate 2	RAC2	21.429
+	2.7821803 07	1.822467 231	Integrin beta-5	ITGB5	88.053
+	1.7451263 25	1.951836 977	Ras-related protein Rab-6A	RAB6A	23.593
+	2.4612761 45	2.339819 089	Integrin alpha-L	ITGAL	128.77
+	2.4911221 73	1.801753 342	Peptidyl-prolyl cis-trans isomerase B	PPIB	23.742
+	2.0634944 52	1.065707 249	Cofilin-1	CFL1	18.502
+	2.4404606 1	1.929039 44	Calreticulin	CALR	48.141

+	1.9288345 28	1.901933 642	Calnexin	CANX	67.567
+	2.6100149 89	1.958949 361	Hematopoietic progenitor cell antigen CD34	CD34	40.716
+	2.0295547 96	1.914144 041	Peroxiredoxin-6	PRDX6	25.035
+	2.7372900 86	2.022460 848	Protein disulfide-isomerase A3	PDIA3	56.782
+	3.0171877 91	1.435732 009	High affinity immunoglobulin epsilon receptor subunit gamma	FCER1G	9.6674
+	2.0404083 63	2.518688 585	Leukocyte elastase inhibitor	SERPINB1	42.741
+	4.2112947 59	1.559662 228	Coronin-1A; Coronin	CORO1A	51.026
+	2.8815493 34	1.228158 409	14-3-3 protein beta/alpha; 14-3-3 protein beta/alpha, N-terminally processed	YWHAB	28.082
+	2.4546446 31	1.039307 513	14-3-3 protein sigma	SFN	27.774
+	5.2049517 15	2.186561 855	Protein S100-A11; Protein S100-A11, N-terminally processed	S100A11	11.74
+	4.7456263 43	2.697921 021	Basigin	BSG	42.2
+	3.3802262 15	1.965906 891	F-actin-capping protein subunit alpha-2	CAPZA2	32.949
+	1.8565391 53	1.515593 133	F-actin-capping protein subunit beta	CAPZB	31.35
+	2.7761128 14	2.225950 068	Regulator of G-protein signaling 19	RGS19	24.635
+	2.7450321 38	1.900179 238	Guanine nucleotide-binding protein G(q) subunit alpha	GNAQ	42.142
+	1.7267892 9	1.838897 245	Vasodilator-stimulated phosphoprotein	VASP	39.829
+	2.1431397 82	1.647704 82	Ras-related protein Rab-7a	RAB7A	23.489
+	1.9708738 71	1.508913 751	Rho GDP-dissociation inhibitor 2	ARHGDIB	22.988
+	2.0485419 29	1.984479 882	F-actin-capping protein subunit alpha-1	CAPZA1	32.922
+	3.8021609 32	2.221259 323	Guanine nucleotide-binding protein G(I)/G(S)/G(O) subunit gamma-2; Guanine nucleotide-binding protein subunit gamma	GNG2	7.8501
+	2.7158979 46	1.329765 813	Triosephosphate isomerase	TPI1	30.791
+	2.1123066 02	1.751722 091	Cell division control protein 42 homolog	CDC42	21.258
+	2.0000940 75	1.355029 129	Ras-related protein Rab-10	RAB10	22.541
+	3.3416152 56	2.397534 886	Actin-related protein 3	ACTR3	47.371
+	1.9118168 29	1.405566 359	ADP-ribosylation factor 1; ADP-ribosylation factor 3	ARF1; ARF3	20.697
+	3.3182635 51	2.262084 585	Transforming protein RhoA	RHOA; RHOC	21.768
+	2.7108881 22	1.407910 456	Beta-2-microglobulin; Beta-2-microglobulin form pl 5.3	B2M	13.714
+	5.4144899 61	3.149060 94	Histone H4	HIST1H4A	11.367
+	2.1216501 91	1.254913 241	Ras-related protein Rab-1A	RAB1A	22.677

+	5.4652388 29	1.714688 881	Guanine nucleotide-binding protein G(I)/G(S)/G(T) subunit beta-1	GNB1	37.377
+	2.5689156 96	2.035149 053	Guanine nucleotide-binding protein G(I)/G(S)/G(T) subunit beta-2	GNB2	37.331
+	2.9618109 17	1.095178 142	Peptidyl-prolyl cis-trans isomerase A;Peptidyl-prolyl cis-trans isomerase A, N-terminally processed;Peptidyl-prolyl cis-trans isomerase	PPIA	18.012
+	3.4426969 43	1.625007 046	Peptidyl-prolyl cis-trans isomerase FKBP1A;Peptidyl-prolyl cis-trans isomerase	FKBP1A	11.951
+	3.2534782 3	2.107771 273	Guanine nucleotide-binding protein G(I)/G(S)/G(O) subunit gamma-5	GNG5	7.3184
+	2.4618347 76	1.765148 807	Elongation factor 1-alpha 1;Putative elongation factor 1-alpha-like 3;Elongation factor 1-alpha	EEF1A1;EEF1A1P5	50.14
+	3.6731629 08	2.815781 566	Histone H3.2;Histone H3.1t;Histone H3.1;Histone H3;Histone H3.3;Histone H3.3C	HIST2H3A;HIST3H3;HIST1H3A;H3F3B;H3F3A;H3F3C	15.388
+	3.4398618 33	3.659429 574	Protein S100-A12;Calcitermin	S100A12	10.575
+	2.6764996 51	1.137638 585	Fatty acid-binding protein, epidermal	FABP5	15.164
+	1.8285094 28	1.391407 495	Adenylyl cyclase-associated protein 1	CAP1	51.901
+	4.5239600 45	2.785394 17	Neuroblast differentiation-associated protein AHNAK	AHNAK	629.09
+	2.0703700 65	2.169972 077	Receptor-type tyrosine-protein phosphatase eta;Protein-tyrosine-phosphatase	PTPRJ	145.94
+	1.8273365 08	2.239621 562	Flotillin-2	FLOT2	47.064
+	2.0173704 11	1.885535 291	Guanine nucleotide-binding protein subunit alpha-13	GNA13	44.049
+	2.0670114 21	1.101183 282	Neutral alpha-glucosidase AB	GANAB	106.87
+	1.9721585 26	1.117567 296	LIM and SH3 domain protein 1	LASP1	29.717
+	1.7443252 14	1.763842 472	Syntaxin-binding protein 2	STXBP2	66.452
+	2.0182134 66	1.514459 377	Ras-related protein Rab-11B	RAB11B	24.488
+	1.9355170 27	1.434445 799	Septin-7		07-Sep 50.679
+	1.8286348 9	1.532713 617	Nucleoside diphosphate kinase;Nucleoside diphosphate kinase B	NME1-NME2;NME2;NME1	32.642
+	1.7008440 02	2.038330 886	Cytoplasmic FMR1-interacting protein 1	CYFIP1	145.18
+	3.0223640 12	1.718125 437	Golgi-associated plant pathogenesis-related protein 1	GLIPR2	17.218
+	2.2827343 66	2.072103 699	EH domain-containing protein 1	EHD1	60.626
+	3.6531087 17	1.513148 634	Guanine nucleotide-binding protein subunit beta-4	GNB4	37.567
+	2.7261015 68	1.791246 612	EH domain-containing protein 3	EHD3	60.886

+	2.1923244 28	1.316610 381	Junctional adhesion molecule A	F11R	32.583
---	-----------------	-----------------	-----------------------------------	------	--------

Table S1 & S2. Significantly upregulated proteins identified by a conservative re-analysis of data obtained from Laurens et al., (2020) regarding proteins detectable in conditioned media of human primary myotubes subject to 24 hours of EPS and Whitham et al., (2018) regarding proteins detected in EVs isolated from human arterial plasma post exercise.